A11101 893074

NAT'L INST OF STANDARDS & TECH R.I.C.

A11101893074

/Bureau of Standards journal of research
QC1 .U5 V3;JL-DE;1929;C.2 C.1 NBS-PUB-C

THE FIRST SPECTRUM OF XENON

By William F. Meggers, T. L. deBruin, and C. J. Humphreys

ABSTRACT

Although 30 years have passed since the discovery of xenon, comparatively little has been known about its spectra, and all attempts to analyze the structure of the Xe_I spectrum have been foiled by the incompleteness and inaccuracy of the available data. This situation has been improved, as follows:

Discharge tubes were filled with pure Xe gas and operated so as to emit only the spectrum of neutral xenon atoms. This spectrum was photographed with quartz-prism and with diffraction grating spectrographs from the ultra-violet to the infra-red. Wave lengths ranging from 3,442.77 to 10,107.2 A have been determined for 318 lines and are supplemented by estimates of relative intensity. Analysis of these new data has resulted in the identification of spectral terms, combinations of which account for practically all of the observed lines.

The normal state of the neutral Xe atom (s^2p^6) is represented by a single level, and successive excited states arise from the addition of *s*-, *p*-, *d*-, *f*- electrons to the xenon ion (s^2p^5). In the notation first introduced to describe the Ne_I spectrum, and subsequently used for A_I, Kr_I, and now also for Xe_I, the single level is called "p_0", and the term groups produced by addition of *s*-, *p*-, *d*-, *f*- electrons are designated "*s*," "*p*," "*d* and *s*," "*x* and *y*," respectively. These groups in the order named theoretically consist of 4, 10, 12, and 12 levels. Each group divides into two subgroups converging in the limit to the two levels of a ^2P term characterizing the normal state of the xenon ion. This subdivision is striking in Kr_I, but especially so in Xe_I on account of the large separation (9,621) of the Xe_{II} doublet.

From the limits of the most regular series in the Xe_I spectrum, and from certain combinations, the absolute value of the $1s_5$ term is established as 30,766.98, and all other term values are based on this one. The resonance lines in the extreme ultra-violet (1,469.61 and 1,295.56 A) then fix the value of the largest term $p_0=$ 97,835 from which the ionization potential of 12.078 volts is deduced for neutral xenon atoms.

CONTENTS

		Page
I.	Introduction	732
II.	Wave-length measurements	734
III.	Analysis of the Xe_I spectrum	736
	1. Theoretical terms	736
	2. Absolute term values; ionization potential of Xe	738
	3. The principal series ($1s_i=mp_k$)	741
	4. The "fundamental" series (*X*, *Y*, *Z*, *U*, *V*, and *W*)	716
	5. The subordinate series	720
	6. The Xe_I spectrum in the extreme ultra-violet	723
	7. Identification of the experimental terms	725
	8. List of Xe_I lines	727

I. INTRODUCTION

Xenon, the heaviest and rarest of the atmospheric gases, was discovered in 1898 by Ramsay and Travers [1] who announced that:

> This gas possesses a spectrum analogous in character to that of argon, but differing entirely in the position of the lines. With the ordinary discharge the gas shows three lines in the red and about five very brilliant lines in the blue; while with the jar and spark gap these lines disappear and are replaced by four brilliant lines in the green, intermediate in position between the two groups of argon lines, the glow in the tube changing from blue to green.

This first reference to the spectrum of xenon points out that there are two entirely different spectra depending on the conditions of excitation, and it has since been the custom to refer to that excited without capacity and external spark gap as the first spectrum, while that produced by a disruptive discharge is called the second spectrum. A prismatic spectrogram showing 15 lines of the second spectrum of xenon was reproduced in color by Ramsay and Travers [2] in 1901. Approximate wave lengths of 250 lines (3,454 to 6,596 A) were published in 1901 by Liveing and Dewar,[3] but this list includes lines of both spectra. The most extensive and accurate descriptions of xenon spectra were published in 1903 by Baly,[4] who measured 92 lines (2,536.58 to 6,198.70 A) in the first spectrum and 1,247 lines (2,414.88 to 6,097.80 A) in the second, a small number of lines being common to both. Eleven of Baly's lines for the first spectrum are identifiable with mercury, so that 81 lines remain in his list (3,469.95 to 6,198.70 A). No extension to Baly's list was made until 1919, when Merrill [5] reported the wave lengths of 54 new lines in the red and infra-red (5,931.2 to 9,162.76 A). Ten strong lines of the first spectrum (4,500.978 to 4,923.246 A) and two of the second (4,603.028 and 4,844.333 A) were measured relative to the primary standard (6,438.4696 A of Cd) by Meggers,[6] and three of the former (4,624.275, 4,671.225, and 4,734.154 A) were also investigated and confirmed by Perard.[7]

Forty-two xenon lines (4,078 to 6,768 A) were examined with Lummer-Gehrcke interferometer plates by Gehrcke and Janicki;[8] they reported fine structure for only two lines, namely, 4,501.13 and 4,734.30 A.

The resonance lines of xenon (1,469.61 and 1,295.56 A) were discovered in 1926 by Hertz and Abbink,[9] and a more extensive investigation of Xe spectra in the extreme ultra-violet was subsequently

---

[1] Ramsay and Travers, Rep. British Assoc., p. 828; 1898.
[2] Ramsay and Travers, Phil. Trans, **A 197**, p. 47; 1901.
[3] Liveing and Dewar, Proc. Roy. Soc., **68**, p. 389; 1901.
[4] Baly, Phil. Trans., **A 202**, p. 183; 1903.
[5] Merrill, B. S. Sci. Paper, **15**, p. 251 (No. 345); 1919.
[6] Meggers, B. S. Sci. Paper, **17**, p. 193 (No. 414); 1921.
[7] Perard, Comptes rendus, **184**, p. 681; 1927.
[8] Gehrcke and Janicki, Ann. d. Phys., **81**, p. 314; 1926.
[9] Hertz and Abbink, Natuurwiss., **14**, p. 648; 1926.

made by Abbink and Dorgelo,[10] who published the wave lengths for 15 lines (1,469.61 to 1,027.04 A) assigned to the first spectrum of Xe.

The electrodeless discharge for xenon was investigated by L. Bloch, E. Bloch, and Déjardin [11] for the purpose of separating successive stages of ionization. Among 1,000 lines, 91 (3,550 to 7,120 A) were assigned to the arc spectrum or first spectrum of xenon (from neutral atoms), and the remaining lines were ascribed to singly, doubly, or trebly ionized atoms. This method of excitation appears to favor the production of spark lines, but it is, in general, a very inefficient source of arc lines. The Zeeman effect of Xe lines has not been investigated at all.

Many attempts have been made to find regularities in the first spectrum of xenon, but on account of inadequate data most of these have failed to yield results of any value. In 1914 Paulson [12] published four triplets, two of which are now known to involve true terms. Sommer [13] arranged 142 lines (including mercury impurity lines) in pairs and groups with 25 wave number differences ranging from 58 to $5{,}840 \pm 3$. It appears that a large majority of these "constant" differences are fortuitous and have no physical significance. Hicks [14] and Williams [15] have also discussed the structure of the first spectrum of xenon, but their results, too, are mostly spurious. Finally, McLennan and Ruedy [16] made absorption experiments with excited xenon gas and found two infra-red lines (8,232 and 8,819 A) to show absorption. Assuming that these lines involved the metastable level s_5, they succeeded in establishing a number of *sp* combinations, but the data available did not permit the assignment of any line to a definite transition.

The above-mentioned attempts to analyze the structure of the Xe_I spectrum emphasize the importance of having a satisfactory description of the spectrum, and our efforts have been directed toward this end in connection with similar work on the Kr_I spectrum.[17]

The purest krypton obtainable contained a trace of xenon, and it was therefore considered advisable to study the xenon spectra also. Furthermore, the practical reason for our study of krypton spectra originates with a proposal to adopt a Kr line as a primary standard of wave length [18] instead of the Cd line now recognized as such. The argument that Kr lines are sharper than Cd lines applies with even greater force to Xe lines with which it is theoretically possible at low temperatures to produce interference phenomena with retarda-

---

[10] Abbink and Dorgelo, Zeit, f. Phys., **47**, p. 221; 1928.
[11] L. Bloch, E. Bloch, Déjardin, Ann. de. Phys. (10), **2**, p. 461; 1924.
[12] Paulson, Astrophys, J., **40**, p. 307; 1914.
[13] Sommer, Zeit. f. Phys., **13**, p. 85; 1923.
[14] Hicks, Phil. Trans., **A 220**, p. 335; 1919.
[15] Williams, Ciencias Fisicas y Matematicas (No. 82), p. 255; 1928.
[16] McLennan and Ruedy, Trans. Roy. Soc. Can. (3), **22**, p. 15; 1928.
[17] Meggers, deBruin and Humphreys, B. S. Jour. Research, **3** (No. 89), p. 129; 1929.
[18] 7 Conf. Gen. Poids et Mesures, p. 52; 1927.

tions of a meter. The possibilities in this direction appear to be worth investigating, and the present paper may be regarded as a contribution to such a program. It is obviously desirable in the first place to describe the first spectrum of xenon with sufficient completeness and accuracy to permit analysis of its structure and classification of its lines. Certain properties of spectral lines are now known to be related to spectral terms (atomic energy levels), so that a classification of the lines enables one to draw upon theoretical considerations in a discussion of their suitability as standards of wave length. The present paper, therefore, deals with a preliminary description and with the interpretation of the Xe_I spectrum. It presents new values for the wave lengths and estimated intensities of 318 lines characterizing neutral xenon atoms and identifies spectral terms which, by their combinations, account for practically all of the observed lines. From the limits of term sequences and from combinations the absolute values of all terms are established. The largest term is $^1S_0$ (p_0) representing the normal state of the neutral xenon atom; its value is 97,835, corresponding to an ionization potential of 12.078 volts. The structure of this spectrum is compared with that of the analogous spectrum of the preceding rare gases, Ne, A, Kr, and a certain grouping of the terms is seen to be associated with the coordination of terms to limits representing the ground levels of the ions. This analysis of the Xe_I spectrum has uncovered additional evidence that *f*-type electrons (in addition to *s*-, *p*-, and *d*- electrons) may play a part in the production of rare gas spectral terms.

It will be desirable to supplement this description and analysis with investigations to record fainter lines and far infra-red lines, to compare the wave lengths of the stronger lines with the primary standard or with the meter itself, to study the hyperfine structure of complex lines, and to observe the Zeeman effects.

II. WAVE-LENGTH MEASUREMENTS

The sources of radiation, spectrographs, and procedure employed in this study of the Xe_I spectrum were almost identical with those described in our report on the Kr_I spectrum, so that it will suffice to give a brief summary of them here. Glass discharge tubes with aluminum disk electrodes like those described by Nutting [19] were filled with remarkably pure Xenon gas purchased from the Linde Gesellschaft für Eismaschinen in Höllriegelskreuth b. München. These tubes were operated on a. c. transformers rated to give 10,000 volts in one case and 40,000 volts in the other. The current in the tube in either case was about 20 milliamperes. The pressure of gas in the tubes and condition of operation was such that an almost

[19] Nutting, B. S. Sci. Papers, 4, p. 511; 1907.

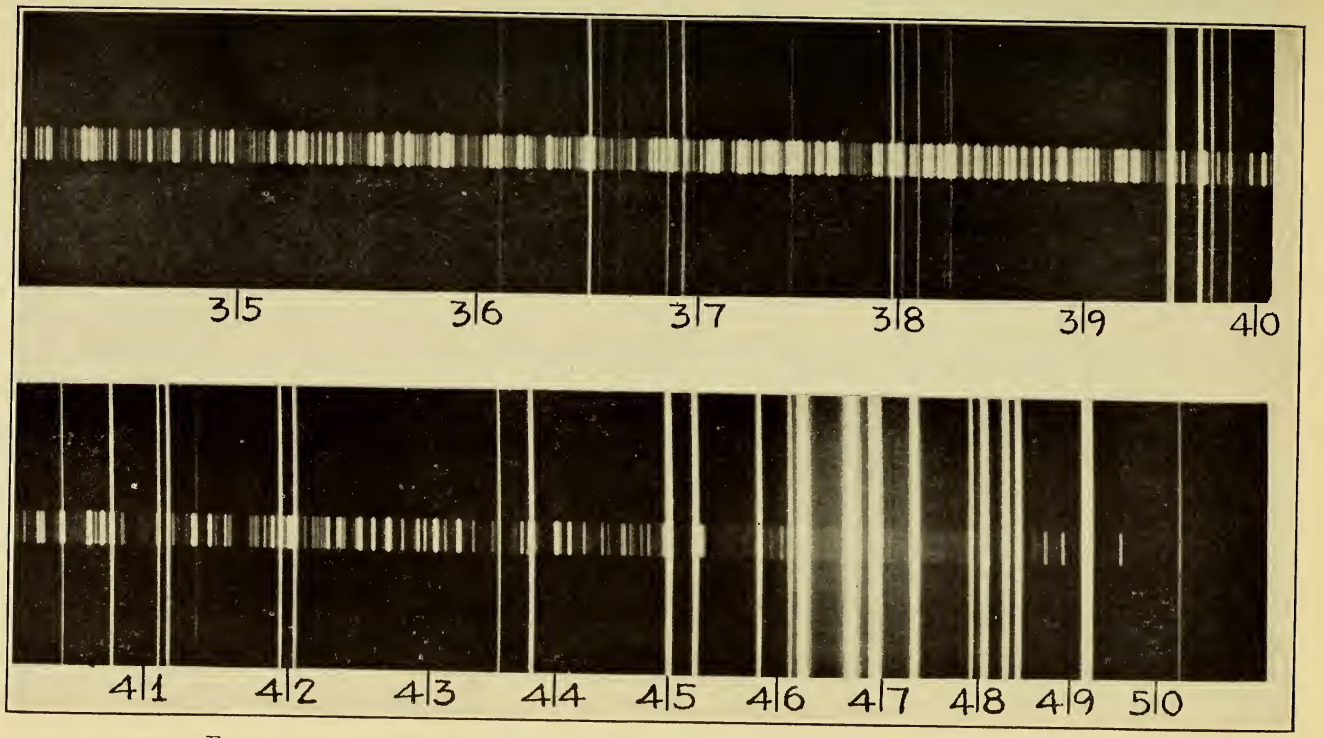

FIGURE 1.—*Arc spectrum of xenon (3500 to 5100 A) with comparison spectrum of iron*

Quartz prism spectrograph

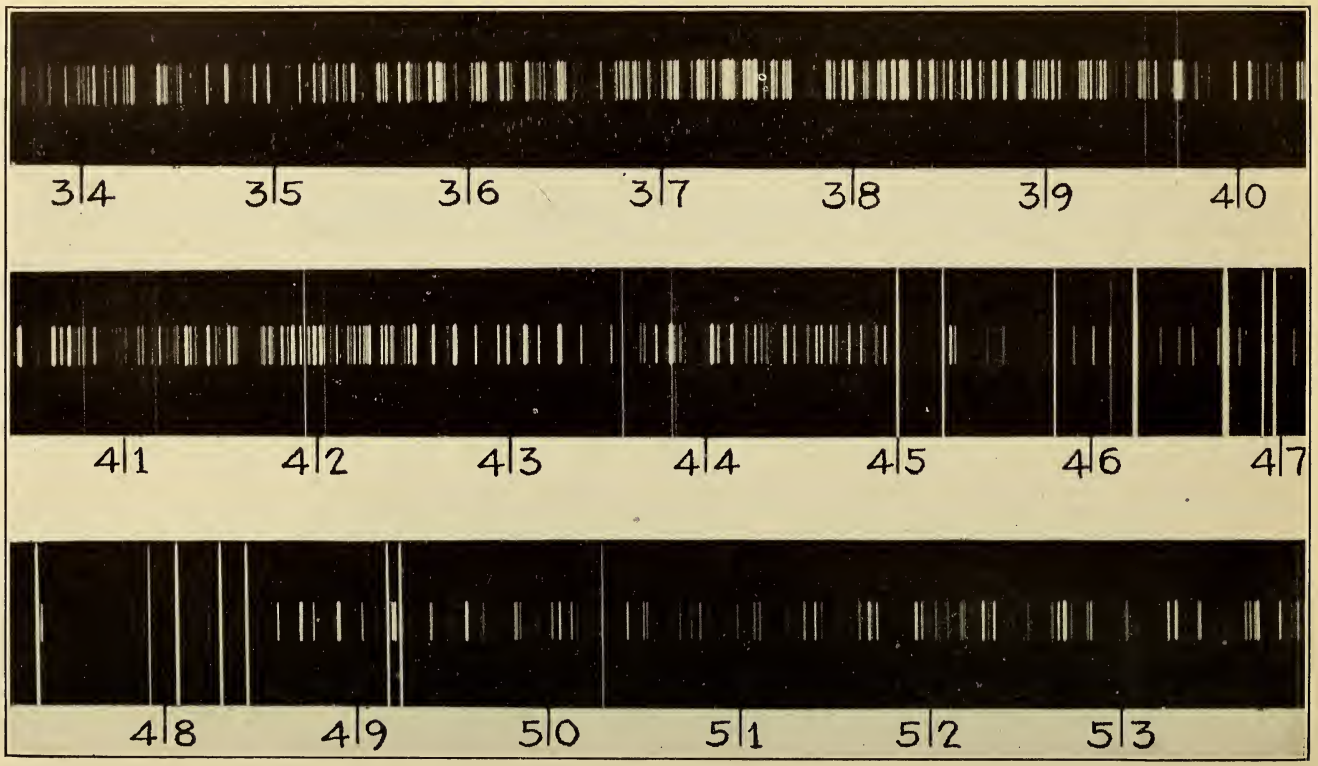

FIGURE 2.—*Arc spectrum of xenon (3400 to 5400 A) with comparison spectrum of iron*

Grating spectrograph

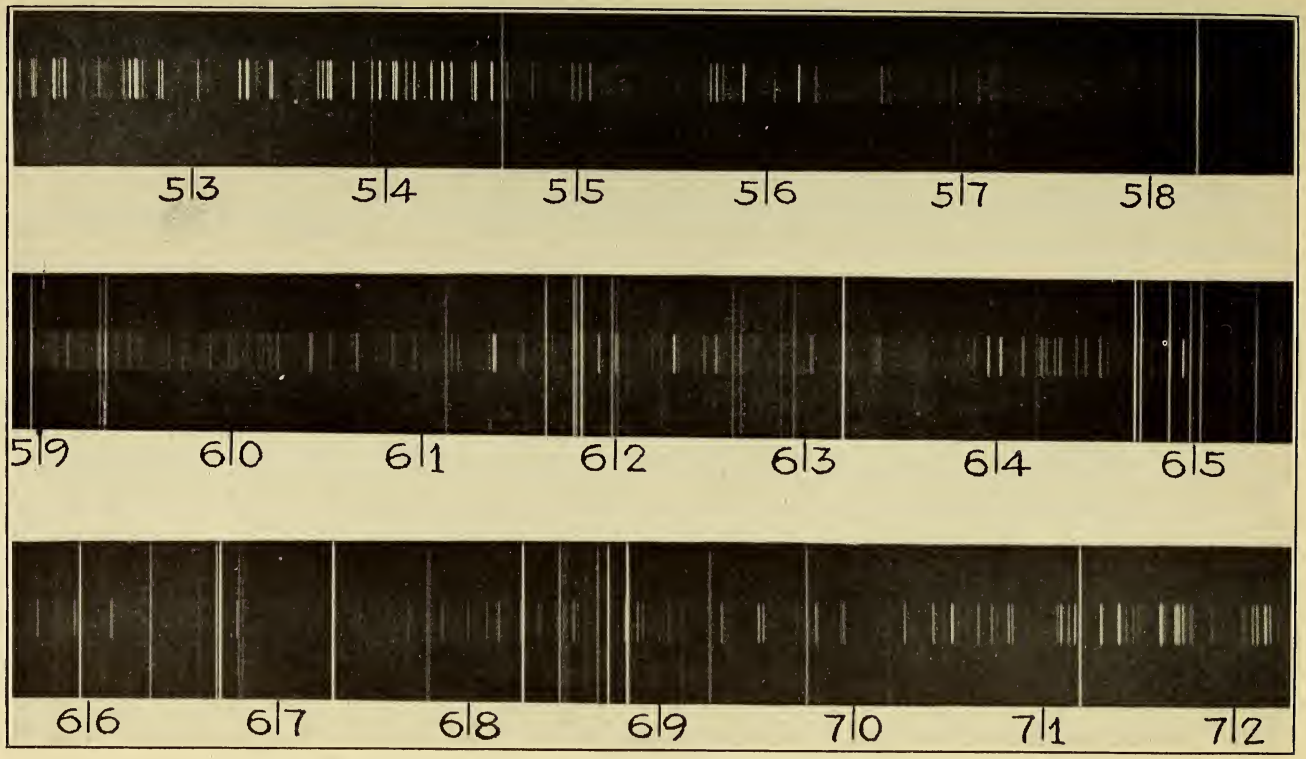

FIGURE 3.—*Arc spectrum of xenon (5300 to 7200 A) with comparison spectrum of iron*

Grating spectrograph

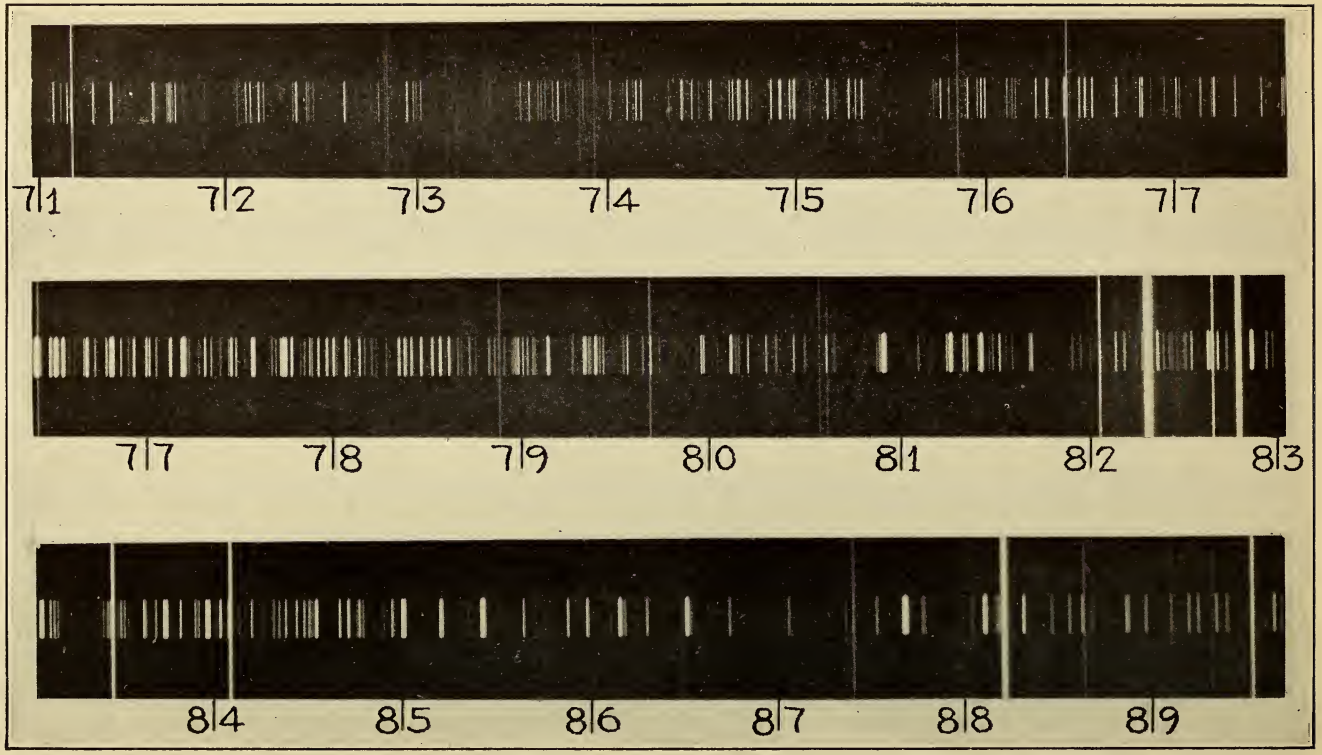

FIGURE 4.—*Arc spectrum of xenon (7100 to 8950 A) with comparison spectrum of iron*

Grating spectrograph

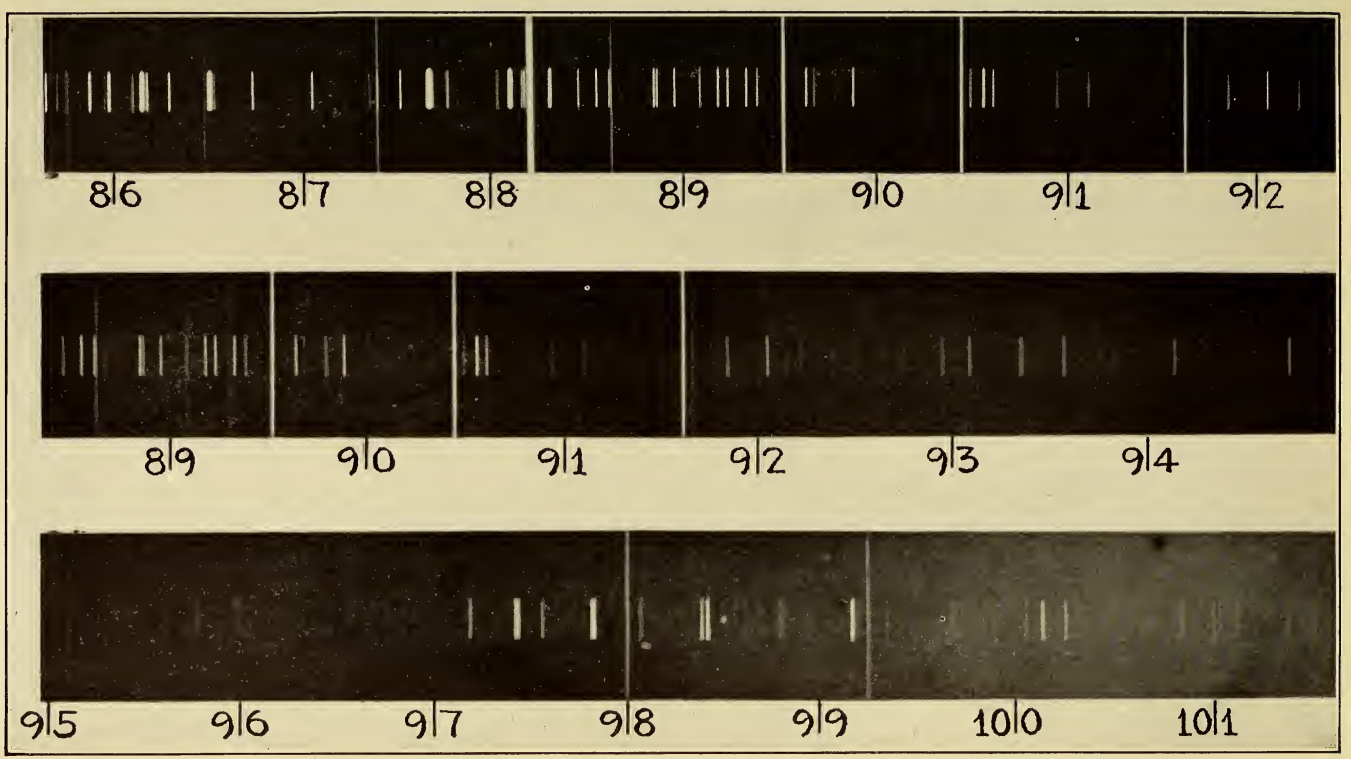

FIGURE 5.—*Arc spectrum of xenon (8600 to 10100 A) with comparison spectrum of iron*

Grating spectrograph

perfectly pure arc spectrum (Xe_I) was emitted, only traces of three or four most intense spark lines (Xe_{II}) showing on the longest exposures. Electrode evaporation occurs when the discharge is passing so that the bulbs are opaque after 10 to 20 hours, but the tubes are good sources of Xe spectra for several hundred hours operation. Most of the spectrograms were made in the first and second order of a 6-inch grating of 21 feet radius of curvature, mounted stigmatically as described before.[20] These were supplemented by several made with a Hilger E_1 autocollimating quartz spectrograph to record faint lines in the ultra-violet end of the spectrum. Eastman's No. 33 photographic plates were used regularly except for the longer wave regions, where No. 36 plates bathed in photosensitizing solutions of dyes were employed. The exposure times ranged from 10 to 48 hours, the latter exposure being sufficient to record a line in the infra-red at 10107.2 A.

Comparison spectra of iron were impressed upon the plates before and after each of the long exposures to xenon and wave-length measurements[21] were made relative to the secondary standards in the spectrum of the iron arc. Most of the lines were measured on four or five spectrograms, and the average probable error of the mean in such cases is not more than one or two hundredths of an Ångstrom unit. Some faint lines were observed only once; that is, on the strongest exposure. The wave lengths of such lines are not given beyond one decimal place. The observed wave lengths, estimated intensities, and term combinations of the Xe_I spectrum are presented in Table 14 at the end of this paper.

Since no complete photographic map of the xenon arc spectrum has ever been published, we are reproducing portions of our spectrograms in Figures 1, 2, 3, 4, and 5. These show the first spectrum of xenon from its limit in the ultra-violet near 3400 A to the infra-red near 10000 A. Xe resembles the preceding rare gases, Ne, A, and Kr, in that its first spectrum consists of groups of very intense lines, one in the blue (4501 to 4923 A) and another beginning at 8206 A in the infra-red and probably extending far beyond the photographic limit. The intervening region is well filled with lines of medium and lower intensity, the strongest visible lines being 5824, 6182, and 6470 A. When the tables of wave length were first compiled, it was rather surprising to find that about 50 per cent more lines were observed for the Xe_I spectrum than for the Kr_I spectrum which was produced and studied in essentially the same manner. The explanation of this superior abundance of Xe_I lines is found in the analysis of the Xe_I spectrum. (See the fundamental series.)

---

[20] Meggers and Burns, B. S. Sci. Papers, **18**, p. 191; 1922.

[21] We are indebted to Bourdon F. Scribner for many of the wave-length computations.

III. ANALYSIS OF THE Xe_I SPECTRUM

1. THEORETICAL TERMS

Neutral xenon ($Z=54$) has in the unexcited state, the atomic configuration of a closed shell with two $5s$- and six $5p$- electrons, symbolized by $5s^2\,5p^6$. The spectral term which characterizes the normal state is a single level, $^1S_0$ according to Hund's theory.[22] The xenon ion, Xe^+, is characterized by the electron group $s^2\,p^5$, giving rise to an inverted doublet term $^2P_{2,1}$[23] in the Xe_{II} spectrum, and the terms representing the excited states of the neutral atom arise from the interaction of the series electron with the s^2p^5 group. The theoretical terms which may be expected to account for the first spectrum of xenon are thus obtained by adding in turn the electrons *ns*, *np*, *nd*, and *nf* to the term ^2P, as shown in Table 1.

TABLE 1.—*Electron configurations and theoretical terms of the Xe_I spectrum*

Electron configuration	Theoretical terms based on $^2P_{2,1}$ of Xe_{II}					Number of levels
$s^2\,p^6$	$^1S_0$					1
$(s^2\,p^5)\,s$	$^1P_1$			$^3P_{2,1,0}$		4
$(s^2\,p^5)\,p$	$^1S_0$ $^1P_1$ $^1D_2$		$^3S_2$	$^3P_{2,1,0}$	$^3D_{3,2,1}$	10
$(s^2\,p^5)\,d$	$^1P_1$ $^1D_2$ $^1F_3$		$^3P_{2,1,0}$	$^3D_{3,2,1}$	$^3F_{4,3,2}$	12
$(s^2\,p^5)\,f$	$^1D_2$ $^1F_3$ $^1G_4$		$^3D_{3,2,1}$	$^3F_{4,3,2}$	$^3G_{5,4,3}$	12

Paschen,[24] in his analysis of the Ne_I spectrum, introduced a special notation for these levels. The set of four levels resulting from the addition of an *s*-electron were called "*s*-terms," s_2, s_3, s_4, s_5 in the order of increasing magnitude. The set of 10 levels was referred to as "*p*-terms," $p_{1,2,3,\text{----}10}$, and the 12 levels from the *d*-electron were represented in part as "*d*-terms" and the remainder as "*s*-terms." Two terms of the following group (originating with an *f*-electron) were recognized and designated as "X- and Y- terms." The same notation was used by Meissner [25] in his analysis of the A_I spectrum and by the authors [26] in their description of the Kr_I spectrum. On account of certain difficulties and uncertainties in the translation of this Paschen notation into the modern quantum symbols, we shall retain the older notation also for the discussion of the Xe_I spectrum. This facilitates intercomparison of these four spectra but it is important to remember that homologous terms in the different spectra may have different inner quantum numbers. In all cases Ne_I, A_I, Kr_I, and Xe_I, the 4 *s*-terms are strictly comparable, but if the 10 *p*-terms

[22] Hund, Linienspektren und periodisches System der Elemente, p. 144, Julius Springer, Berlin; 1927.

[23] For convenience in printing and reading the inner quantum numbers of levels belonging to even multiplicities are increased by one-half.

[24] Paschen, Ann. d. Phys., **60**, p. 405; 1919; **63**, p. 201; 1920.

[25] Meissner, Zeit. f. Phys., **27**, p. 238; 1926; **39**, p. 172; 1926; **40**, p. 839; 1927.

[26] Meggers, de Bruin and Humphreys, B. S. Jour. Research, **3** (No. 89), p. 129; 1929.

are numbered (with subscripts) in order of magnitude they must be rearranged to compare levels with the same inner quantum numbers as shown in Table 2.

TABLE 2.—*Corresponding terms in Ne_I, A_I, Kr_I, and Xe_I spectra*

j	0	1	0	2	1	2	1	2	3	1	1	0	1	2
NeI	p_1	p_2	p_3	p_4	p_5	p_6	p_7	p_8	p_9	p_{10}	s_2	s_3	s_4	s_5
AI	p_1	p_2	p_5	p_3	p_4	p_6	p_7	p_8	p_9	p_{10}	s_2	s_3	s_4	s_5
KrI	p_1	p_3	p_5	p_2	p_4	p_6	p_7	p_8	p_9	p_{10}	s_2	s_3	s_4	s_5
XeI	p_1	p_2	p_5	p_3	p_4	p_6	p_7	p_9	p_8	p_{10}	s_2	s_3	s_4	s_5

In each case it has been found that the group of terms may be divided into subgroups converging to two limits separated by a "displacement constant," A. The limits are the two ground levels, $^2P_2$ and $^2P_1$ of the ion. The displacement constant, A, found from the limits of the Ritzian and non-Ritzian series, is related to the coordination of the arc spectrum levels to the two levels $^2P_{2,1}$ of the ion and is approximately the same magnitude as the separation of these levels. The data for the four rare gas spectra are given in Table 3.

TABLE 3.—*Displacement constants and level separations in rare gas spectra*

	Neon	Argon	Krypton	Xenon
A	780. 0	1, 423. 20	5, 330±	Vide infra.
$^2P_{2,1}$	782	1, 431	5, 371	9, 621
$1s_5$-$1s_3$ / $^3P_2$-$^3P_0$	776. 90	1, 409. 92	5, 219. 90	9, 129. 24
Centers of gravity of $3p$-term groups	788	1, 451	5, 353	Vide infra.

On account of the very large separation of $^2P_{2,1}$ for xenon, it is impossible to find any but the first members of the non-Ritzian sequence $np_{1,2,3,4}$, since the second members would give negative term values. It is therefore not possible to determine the displacement constant A of xenon from the series limits. However, an upper limit can be found from the distance between centers of gravity of the $^2p_{5,6}$ ----10 and the $^2p_{1,2,3,4}$ groups. This upper limit has the value 10,540. The lower limit for this A is the $1s_5$-$1s_3$ separation, which amounts to 9,129.24. The $^2P_{2,1}$ separation in Xe_{II} has been found [27] to be 9,621, which is in satisfactory agreement with the two limits 9,129 and 10,540 just discussed. For calculating the effective quantum numbers of the non-Ritzian Xe_I terms we have assumed A = 9,621.

[27] Humphreys and deBruin, Sci., **68**, p. 573; 1928.

2. ABSOLUTE TERM VALUES; IONIZATION POTENTIAL OF Xe

Among the various series identified in Ne_I, A_I, and Kr_I spectra, one, namely, $2p_9$-md_4', was unique in the regularity of its effective quantum numbers. The analogous series in Xe_I is $2p_8$-md_4', and again it is the most regular as well as the longest. As in the preceding cases, this series has been employed for the determination of absolute term values, since it is probable that the best values must result from extrapolation of the longest series following most closely a Ritz formula. The $2p_8$-md_4' series fixes the level $2p_8=19{,}431.49$, and addition of the wave number $1s_5$-$2p_8=11{,}335.49$, places the $1s_5$ level at 30,766.98. The same level can be arrived at independently from several different series. The results are summarized as follows:

1. Series $2p_8$-md_4' and $1s_5$-$2p_8$	$1s_5=30{,}766.98$
2. Series $2p_9$-md_4 and $1s_5$-$2p_9$	$1s_5=30{,}768.26$
3. Series $2p_6$-md_1' and $1s_5$-$2p_6$	$1s_5=30{,}767.61$
4. Series $1s_3$-mX and $1s_5$-$1s_3$	$1s_5=30{,}766.12$
5. Series $1s_5$-mp_6	$1s_5=30{,}767.24$
6. Series $1s_5$-mp_8	$1s_5=30{,}765.28$

The mean of the six values is 30,766.91, practically identical with the first one, which is chosen as the basic value. All remaining term values are relative to $1s_5=30{,}766.98$, and any error in this level is therefore the same for all the other terms. The details of the above-mentioned calculations of $1s_5$ are presented in Table 4.

TABLE 4.—*Determination of absolute term values*

Series $2p_8$-md_4'

$$\nu = A - \frac{R}{[m+\mu+\alpha(A-\nu)]^2}$$

$R_{xe} = 109{,}736.66$
$A = 19431.489$
$\alpha = -0.000001377271113$
$\mu = +0.5197276575 \pm 10^{-10}$

m	Int.	$\lambda_{obs.}$	$\nu_{obs.}$	$\nu_{calc.}$	ν obs.− ν calc.
2				[a] 1, 809. 645	
3	3	9, 513. 33	10, 508. 71	10, 511. 369	−2. 66
4	30	7, 119. 58	14, 041. 91	14, 041. 910	0. 00
5	30	6, 318. 08	15, 823. 22	15, 823. 220	0. 00
6	8	5, 934. 14	16, 846. 98	16, 847. 045	−0. 06
7	3	5, 716. 14	17, 489. 48	17, 489. 456	+0. 02
8	1	5, 579. 16	17, 918. 88	17, 918. 929	−0. 05
9	1−	5, 486. 90	18, 220. 18	18, 220. 180	0. 00

$$2p_8 = 19{,}431.489$$
$$1s_5 - 2p_8 = 11{,}335.49$$
$$1s_5 = 30{,}766.98$$

Series $2p_9$-md_4

$A = 19{,}716.015$
$\alpha = +0.000006775882325$
$\mu = +0.5392837788 \pm 10^{-10}$

m	Int.	$\lambda_{obs.}$	$\nu_{obs.}$	$\nu_{calc.}$	ν obs.− ν calc.
2				4, 036. 67	
3	5	9, 167. 47	10, 905. 14	11, 233. 42	−328. 28
4	60	6, 882. 15	14, 526. 35	14, 472. 71	+53. 64
5	20	6, 182. 41	16, 170. 45	16, 170. 45	0. 00
6	4	5, 824. 76	17, 163. 33	17, 163. 33	0. 00
7	2	5, 618. 80	17, 792. 47	17, 792. 08	+0. 39
8	1−	5, 488. 56	18, 214. 69	18, 214. 69	0. 00
9	1−	5, 400. 4	18, 512. 01	18, 512. 15	−0. 14

$$2p_9 = 19{,}716.015$$
$$1s_5 - 2p_9 = 11{,}052.25$$
$$1s_5 = 30{,}768.26$$

[a] Exact calculation given on p. 748.

TABLE 4.—*Determination of absolute term values*—Continued

Series $2p_6$-md_1'

$A=18{,}622.663$
$\alpha=+0.000002752635528$
$\mu=+0.6180082686\pm10^{-10}$

m	Int.	$\lambda_{obs.}$	$\nu_{obs.}$	$\nu_{calc.}$	ν obs.− ν calc.
2				3, 121. 40	
3	2	9, 685. 29	10, 322. 11	10, 344. 02	−21. 91
4	6	7, 393. 77	13, 521. 19	13, 508. 22	+12. 97
5	20	6, 595. 54	15, 157. 85	15, 157. 85	0. 00
6	4	6, 200. 86	16, 122. 35	16, 122. 35	0. 00
7	2	5, 974. 08	16, 734. 35	16, 734. 34	+0. 01
8	1	5, 830. 47	17, 146. 52	17, 146. 52	0. 00
9	1−	5, 733. 4	17, 436. 83	17, 437. 20	−0. 37

$$2p_6=18{,}622.663$$
$$1s_5-2p_6=12{,}144.95$$
$$1s_5=30{,}767.61$$

Series $1s_3$-mX

$A=21{,}636.880$
$\alpha=+0.000002293149515$
$\mu=+0.9439590749\pm10^{-10}$

m	Int.	$\lambda_{obs.}$	$\nu_{obs.}$	$\nu_{calc.}$	ν obs.− ν calc.
3	40	6, 827. 30	14, 643. 04	14, 639. 10	+3. 94
4	15	5, 823. 89	17, 165. 90	17, 165. 90	0. 00
5	4	4, 392. 74	18, 538. 30	18, 538. 30	0. 00
6	2	5, 162. 66	19, 364. 48	19, 364. 48	0. 00
7	1−	5, 023. 80	19, 899. 71	19, 899. 71	0. 00

$$1s_3=21{,}636.880$$
$$1s_5-1s_3=9{,}129.24$$
$$1s_5=30{,}766.12$$

Series $1s_5-mp_6$

$A=30{,}767.237$
$\alpha=-0.000003114322468$
$\mu=+0.4985618368\pm10^{-10}$

m	Int.	$\lambda_{obs.}$	$\nu_{obs.}$	$\nu_{calc.}$	ν obs.− ν calc.
2	300	8, 231. 62	12, 144. 95	12, 353. 55	−208. 60
3	150	4, 624. 29	21, 618. 90	21, 654. 54	−35. 64
4	15	3, 950. 92	25, 303. 42	25, 303. 42	0. 00
5	3	3, 685. 91	27, 122. 65	27, 122. 65	0. 00
6	1	3, 549. 84	28, 162. 27	28, 162. 27	0. 00
7	1−	3, 469. 96	28, 810. 56	28, 812. 44	−1. 88

$$1s_5=30{,}767.24$$

TABLE 4.—*Determination of absolute term values*—Continued

Series $1s_5-mp_8$

$A=30{,}765.284$
$\alpha=-0.000004234844672$
$\mu=+0.4630334435\pm10^{-10}$

m	Int.	$\lambda_{obs.}$	$\nu_{obs.}$	$\nu_{calc.}$	ν obs.− ν calc.
2	200	8, 819. 43	11, 335. 49	11, 409. 57	−74. 08
3	300	4, 671. 22	21, 401. 71	21, 401. 71	0. 00
4	20	3, 967. 55	25, 197. 37	25, 197. 37	0. 00
5	3	3, 963. 51	27, 066. 84	27, 067. 19	−0. 35
6	1	3, 554. 03	28, 129. 07	28, 129. 07	0. 00
7	1−	3, 472. 49	28, 790. 06	28, 790. 61	−0. 55

$1s_5=30{,}765.28$

The resonance lines of xenon lie in the extreme ultra-violet at 1469.61 and 1295.56 A. They form the connecting link between the ground term p_0 ($^1S_0$) and the excited states $1s_2$ and $1s_4$ ($^1P_1$ and $^3P_1$), and permit the evaluation of this largest term, and calculation of the ionization potential. Thus, from the terms $1s_4=29{,}789.34$ and $1s_2=20{,}649.44$, we obtain:

$$p_0-1s_4=1469.61 \text{ A};\ \nu=68{,}045.3;\ p_0=97{,}834.6$$
$$p_0-1s_2=1295.56 \text{ A};\ \nu=77{,}186.7;\ p_0=97{,}836.1$$

The final value of the normal state of neutral xenon atoms is therefore

$$p_0\ (^1S_0)=97{,}835.3$$

corresponding to an ionization potential of 12.078 volts. This is in good agreement with the estimation of Abbink and Dorgelo [28] on the absorption of spark lines (ca. 12.0 volts) but somewhat higher than the value obtained by Hertz and Kloppers [29] from critical potential measurements (ca. 11.5 volts).

3. THE PRINCIPAL SERIES $1s_i$-mp_k

The data for the 10 principal series $1s_i$-mp_k are presented in Table 5, where the observational data are represented by estimated intensity of the spectral line (in parenthesis) followed by the measured wave length λ. The corresponding wave number in vacuum, ν, was computed with the aid of Kayser's "Tabelle der Schwingungszahlen," except for lines in the unexplored infra-red region which are represented by term differences. Values of mp have been calculated from each combination, and finally the mean value of each term and the effective quantum number $\sqrt{\frac{R}{mp}}$, associated with it are given.

[28] Abbink and Dorgelo, Zeit. f. Phys., **47**, p. 232; 1928.
[29] Hertz and Kloppers, Zeit. f. Phys., **31**, p. 403; 1925.

TABLE 5.—*Xe principal series, $1s_i$-m_k*

Series, mp_1

Limits: $1s_2=20{,}649.44$
$1s_4=29{,}789.34$

Comb.	m	λ
s_2p_1	λ	(8)7, 887. 38
	ν	12, 675. 00
	mp_1	7, 974. 44
s_4p_1	λ	(30)4, 582. 74
	ν	21, 814. 92
	mp_1	7, 974. 42
Mean	mp_1	7, 974. 43
	$\sqrt{\frac{R}{mp_1+A}}$	2. 4973

$A=9{,}621$

Series, mp_2

Limits: $1s_2=20{,}649.44$
$1s_3=21{,}637.74$
$1s_4=29{,}789.34$
$1s_5=30{,}766.98$

Comb.	m	λ
s_2p_2	λ	(20)8, 266. 53
	ν	12, 093. 65
	mp_2	8, 555. 79
s_3p_2	λ	(15)7, 642. 02
	ν	13, 081. 95
	mp_2	8, 555. 79
s_4p_2	λ	(2)4, 708. 19
	ν	21, 233. 66
	mp_2	8, 555. 68
s_5p_2	λ	(100)4,500.99
	ν	22, 211. 12
	mp_2	8, 555. 86
Mean	mp_2	8, 555. 78
	$\sqrt{\frac{R}{mp_2+A}}$	2. 4571

$A=9{,}621$

TABLE 5.—*Xe principal series, $1s_i$-m_k*—Continued

Series, mp_3

Limits: $1s_2=20{,}649.44$
$1s_4=29{,}789.34$
$1s_5=30{,}766.98$

Comb.	m	?
s_2p_3	λ	(50)8, 346. 86
	ν	11, 977. 26
	mp_3	8, 672. 18
s_4p_3	λ	(100)4, 734. 15
	ν	21, 117. 23
	mp_3	8, 672. 21
s_5p_3	λ	(50)4, 524. 68
	ν	22, 094. 83
	mp_3	8, 672. 15
Mean	mp_3	8, 672. 18
	$\sqrt{\frac{R}{mp_3+A}}$	2. 4492

$A=9{,}621$

Series, mp_4

Limits: $1s_2=20{,}649.44$
$1s_3=21{,}637.74$
$1s_4=29{,}789.34$
$1s_5=30{,}766.98$

Comb.	m	?
s_2p_4	λ	(5)8, 930. 81
	ν	11, 194. 03
	mp_4	9, 455. 41
s_3p_4	λ	(25)8, 206. 34
	ν	12, 182. 36
	mp_4	9, 455. 38
s_4p_4	λ	(50)4, 916. 50
	ν	20, 334. 01
	mp_4	9, 455. 33
s_5p_4	λ	(25)4, 690. 97
	ν	21, 311. 61
	mp_4	9, 455. 37
Mean	mp_4	9, 455. 37
	$\sqrt{\frac{R}{mp_4+A}}$	2. 3984

$A=9{,}621$

NOTE.—The use of 6-point type for the remaining series does not reflect on their importance.

TABLE 5.—*Xe principal series, $1s_i$-m_k*—Continued

Series, mp_5
Limits: $1s_2$=20,649.44
$1s_4$=29,789.34

Comb.	m	2	3	4	5	6
s_2p_5	λ		(5)8, 576. 03	(15d)6, 504. 16		
	ν	2, 933. 85	11, 657. 21	15, 370. 54		
	mp_5	17, 715. 59	8, 992. 23	5, 278. 90		
s_4p_5	λ	(150)8, 280. 16	(100)4, 807. 01	(20)4, 078. 81	(4)3, 809. 90	(2)3, 669. 94
	ν	12, 073. 75	20, 797. 16	24, 510. 06	26, 239. 99	27, 240. 67
	mp_5	17, 715. 59	8, 992. 18	5, 279. 28	3, 549. 35	2, 548. 67
Mean	mp_5	17, 715. 59	8, 992. 20	5, 279. 09	3, 549. 35	2, 548. 67
	$\sqrt{\frac{R}{mp_5}}$	2. 4888	3. 4933	4. 5593	5. 5604	6. 5618

Series, mp_6
Limits: $1s_2$=20,649.44
$1s_4$=29,789.34
$1s_5$=30,766.98

Comb.	m	2	3	4	5	6	7
s_2p_6	λ		(3)8, 692. 08	(3)6, 583. 15			
	ν	2, 027. 40	11, 501. 57	15, 186. 11			
	mp_6	18, 622. 04	9, 147. 87	5, 463. 33			
s_4p_6	λ	(50)8, 952. 25	(60)4, 843. 29	(10)4, 109. 71	(2)3, 823. 76	(4)3, 677. 62	
	ν	11, 167. 31	20, 641. 37	24, 325. 78	26, 144. 88	27, 183. 79	
	mp_6	18, 622. 03	9, 147. 97	5, 463. 56	3, 644. 46	2, 605. 55	
s_5p_6	λ	(300)8, 231. 64	(200)4, 624. 29	(20)3, 950. 92	(4)3, 685. 91	(2)3, 549. 84	(1)3, 469. 96
	ν	12, 144. 92	21, 618. 90	25, 303. 43	27, 122. 65	28, 162. 27	28, 810. 55
	mp_6	18, 622. 06	9, 148. 06	5, 463. 55	3, 644. 33	2, 604. 71	1, 956. 43
Mean	mp_6	18, 622. 04	9, 147. 97	5, 463. 48	3, 644. 40	2, 604. 93	1, 956. 43
	$\sqrt{\frac{R}{mp_6}}$	2. 4275	3. 4635	4. 4817	5. 4874	6. 4905	7. 4893

Series, mp_7
Limits: $1s_2$=20,649.44
$1s_3$=21,637.74
$1s_4$=29,789.34
$1s_5$=30,766.98

Comb.	m	2	3	4	5	6
s_2p_7	λ		(6)8, 648. 51			
	ν	1, 770. 94	11, 559. 51			
	mp_7	18, 878. 50	9, 089. 93			
s_3p_7	λ		(10)7, 967. 33			
	ν	2, 759. 24	12, 547. 81			
	mp_7	18, 878. 50	9, 089. 93			
s_4p_7	λ	(40)9, 162. 66	(70)4, 829. 71	(15)4, 116. 11	(3)3, 826. 86	(1)3, 679. 31
	ν	10, 910. 87	20, 699. 41	24, 287. 95	26, 123. 70	27, 171. 30
	mp_7	18, 878. 47	9, 089. 93	5, 501. 39	3, 665. 64	2, 618. 04
s_5p_7	λ	(60)8, 409. 21	(8)4, 611. 88	(1)3, 956. 88		
	ν	11, 888. 46	21, 677. 08	25, 265. 31		
	mp_7	18, 878. 52	9, 089. 90	5, 501. 67		
Mean	mp_7	18, 878. 50	9, 089. 92	5, 501. 53	3, 665. 64	2, 618. 04
	$\sqrt{\frac{R}{mp_7}}$	2. 4110	3. 4743	4. 4661	5. 4714	6. 4742

TABLE 5.—*Xe principal series, $1s_i$-m_k*—Continued

Series, mp_8
Limit: $1s_5$=30,766.98

Comb.	m	2	3	4	5	6	7
s_5p_8	λ	(200)8,819.44	(300)4,671.22	(30)3,967.55	(5)3,693.50	(2)3,554.03	(1)3,472.43
	ν	11,335.47	21,401.71	25,197.37	27,066.92	28,129.07	28,790.06
	mp_8	19,431.51	9,365.27	5,569.61	3,700.06	2,637.91	1,976.92
Mean	mp_8	19,431.51	9,365.27	5,569.61	3,700.06	2,637.91	1,976.92
	$\sqrt{\frac{R}{mp_8}}$	2.3764	3.4231	4.4388	5.4459	6.4498	7.4504

Series, mp_9
Limits: $1s_2$=20,649.44
$1s_4$=29,789.34
$1s_5$=30,766.98

Comb.	m	2	3	4	5
s_2p_9	λ		(50)8,952.25		
	ν	934.72	11,167.31		
	mp_9	19,714.72	9,482.13		
s_4p_9	λ	(10)9,923.10	(60)4,923.15	(4)4,135.12	
	ν	10,074.74	20,306.55	24,176.30	
	mp_9	19,714.60	9,482.79	5,613.04	
s_5p_9	λ	(50)9,045.46	(70)4,697.02	(5)3,974.42	(1)3,696.82
	ν	11,052.24	21,284.16	25,153.81	27,042.61
	mp_9	19,714.74	9,482.82	5,613.17	3,724.37
Mean	mp_9	19,714.72	9,482.80	5,613.1	3,724.37
	$\sqrt{\frac{R}{mp_9}}$	2.3593	3.4018	4.4216	5.4281

Series, mp_{10}
Limits: $1s_2$=20,649.44
$1s_3$=21,637.74
$1s_4$=29,789.34
$1s_5$=30,766.98

Comb.	m	2	3	4	5
s_2p_{10}	λ		(1)9,306.56	(4)6,678.94	(1)5,921.79
	ν	84.11	10,724.17	14,968.31	16,882.12
	mp_{10}	20,565.33	9,907.27	5,681.13	3,767.32
s_3p_{10}	λ		(2)8,522.49	(4)6,265.28	(1)5,594 21
	ν	1,072.41	11,730.44	15,956.57	17,870.68
	mp_{10}	20,565.33	9,907.30	5,681.17	3,767.06
s_4p_{10}	λ		(15)5,028.26		
	ν	9,224.01	19,882.07		
	mp_{10}	20,565.33	9,907.27		
s_5p_{10}	λ	(20)9,799.65	(20)4,792.61	(5)3,985.22	(1)3,702.72
	ν	10,201.65	20,859.64	25,085.65	26,999.52
	mp_{10}	20,565.33	9,907.34	5,681.33	3,767.46
Mean	mp_{10}	20,565.33	9,907.29	5,681.21	3,767.26
	$\sqrt{\frac{R}{mp_{10}}}$	2.3100	3.3281	4.3950	5.3972

From Table 5 it can readily be seen that the 10 principal series, $1s_1$-mp_k, are separated into two groups, $p_{1,2,3,4}$ going to the higher level $^2P_1$ of the ion, and $p_{5,6,7,8,9,10}$ to the lower level $^2P_2$. In the Kr_I analysis we were able to establish two members of the non-

Ritzian series, but in Xe_I only the first members can be obtained, since, on account of the very large displacement constant A, the second members will have negative term values.

No lines of the principal series can be expected shorter than 3249 A, and between this limit and the resonance line at 1469 A, no Xe_I lines can be produced. The longest wave length of the principal series in the Xe_I spectrum is given by the combination $1s_2-2p_{10}=84.11$, corresponding to a wave length of 1,188,919 A = 118.8919 μ = 1/8 mm (approximately).

4. THE "FUNDAMENTAL" SERIES (X, Y, Z, U, V, AND W)

Paschen found two unidentified terms, x and y, in the Ne_I spectrum and when Messiner found three similar terms in the A_I spectrum, he called them X, Y, and Z. Meissner [30] pointed out that these series begin with order number $m=4$, are hydrogen-like, and might, therefore, be regarded as f-terms. Since, however, these terms combined with s- and d-terms but not with p-terms, the simple selection rule $\Delta\ l=\pm 1$ was violated and it was necessary to hold in reserve the final interpretation of these f-type terms.

The authors also found two series, X and Y, in the Kr_I spectrum, and interpreted them as terms arising from the configuration $(s^2\ p^5)\ f$. We now feel certain that this is the correct explanation, because we have found this term group much more fully developed in the Xe_I spectrum. In fact, 6 series and 34 terms belonging to the $(s^2\ p^5)\ f$ configuration have been detected in Xe_I; the X and Y series combinations with s-terms are presented in Table 6.

TABLE 6.—*Xe_I fundamental series, $1s_i$-mf_k*

SERIES, mX

Limits: $1s_2=20{,}649.44$
$1s_3=21{,}637.74$
$1s_4=29{,}789.34$
$1s_5=30{,}766.98$

Comb.	m	4	5	6	7	8	9
s_2X	λ	(5)7,321.46	(7)6,179.66	(3)5,696.44	(1)5,440.2	(1)5,286.1	(1−)5,185.33
	ν	13,654.73	16,177.65	17,549.96	18,376.58	18,912.29	19,279.82
	mX	6,994.71	4,471.79	3,099.48	2,272.86	1,737.15	1,369.62
s_3X	λ	(40)6,827.30	(20)5,823.89	(4)5,392.74	(2)5,162.66	(1)5,023.84	
	ν	14,643.04	17,165.91	18,538.31	19,364.48	19,899.56	
	mX	6,994.70	4,471.83	3,099.43	2,273.26	1,738.18	
s_4X	λ	(10)4,385.75	(1)3,948.70				
	ν	22,794.73	25,317.65				
	mX	6,994.61	4,471.69				
s_5X	λ	(3)4,205.37					
	ν	23,772.45					
	mX	6,994.53					
Mean	mX	6,994.68	4,471.82	3,099.40	2,273.04	1,737.83	1,369.62
	$\sqrt{\frac{R}{mX}}$	3.9609	4.9538	5.9503	6.9482	7.9464	8.9510

[30] Meissner, Zeit. f. Phys., 39, p. 178; 1926.

TABLE 6.—*Xe_I fundamental series, $1s_i$-mf_k*—Continued

SERIES mY

Limits: $1s_2$=20,649.44
$1s_4$=29,789.34
$1s_5$=30,766.98

Comb.	m	4	5	6	7	8	9
s_2Y	λ	(5)7,316.28	(9)6,178.30	(5)5,695.74	(1)5,440.2	(1)5,286.1	(1−)5,185.33
	ν	13,664.39	16,181.21	17,552.12	18,377.60	18,912.29	19,279.82
	mY	6,985.05	4,468.23	3,097.32	2,271.84	1,737.15	1,369.62
s_4Y	λ	(15)4,383.90	(5)3,948.19	(2)3,745.44	(2)3,633.15		
	ν	22,804.35	25,320.92	26,691.57	27,516.51		
	mY	6,984.99	4,468.42	3,097.77	2,272.83		
s_5Y	λ	(10)4,203.69	(3)3,801.43	(2)3,613.07			
	ν	23,781.95	26,298.45	27,669.43			
	mY	6,985.03	4,468.53	3,097.55			
Mean	mY	6,985.03	4,468.35	3,097.50	2,272.14	1,737.15	1,369.62
	$\sqrt{\frac{R}{mY}}$	3.9636	4.9557	5.9521	6.9496	7.9480	8.9510

These X and Y series are hydrogenlike in every case and may, therefore, be called "fundamental" to distinguish them from "principal" and "subordinate" series. The terms of the f-series have nearly the same value in different rare-gas spectra, tending to increase slightly with heavier atoms. The first members of the X and Y series (and effective quantum numbers) in different spectra are compared in Table 7, to which is added a comparison of the values for the $3d_4'$ term. It is seen that the 12 d-terms arising from the $(s^2p^5)\,3d$ configuration assume a relatively deeper position in the energy diagram as we pass from lighter to heavier atoms. This is exemplified by the increase of $3d_4'$ from 12,339 in Ne_I to 17,636 in Xe_I. The md-mf combinations in Ne_I, A_I, and Kr_I fall in the infra-red outside of the range of photographic investigation, but in Xe_I, on account of the larger interval between the d- and f-terms, it was possible to observe the $3d$-mf combinations. This explains why we observed about 50 per cent more lines in Xe_I than in Kr_I although essentially the same procedure was used in both. These combinations may be expected to be even more prominent in the spectrum of Radon.

TABLE 7.—*Comparison of d- and f-terms in rare-gas spectra*

	Ne_I	A_I	Kr_I	Xe_I	Rn_I
$4X$ (f_6)	6,876.73	6,922.91	6,950.21	6,994.68	(7,000±)
n_{eff}	3.9940	3.9813	3.9726	3.9609	?
$4Y$ (f_5)	6,860.23	6,881.55	6,893.68	6,985.03	(7,000±)
n_{eff}	3.9988	3.9933	3.9896	3.9636	?
$3d_4'$	12,339.15	14,362.0	(15,400±)	17,636.85	(20,000±)
n_{eff}	2.9816	2.7642	(2.6694)	2.4944	?

It is quite probable that some of the unidentified A_I and Kr_I lines in the infra-red are combinations of this type. The $(s^2\ p^5)\ f$ terms combine with the terms arising from $(s^2\ p^5)\ 1s$ and from $(s^2\ p^5)\ 3d$ as shown in Table 8. These combinations, as well as the analogous ones in the Ne_I, A_I and Kr_I spectra, are in perfect accord with the revised rules governing transitions when two or more electrons are involved.[31] Transitions occur for which the l of one electron changes ± 1 while the l of another changes 0 or ± 2. In other words, transitions occur only when the sum of all changes in l is odd. Thus, the sf combinations may be interpreted as double electron jumps in which the s electron makes a transit to a p orbit ($\Delta l = 1$) while the p electron is passing to an f orbit ($\Delta l = 2$).

The series $3d_4'$-mZ and $3d_1''$-mZ can be used for the calculation of the term values $3d_4'$ and $3d_1''$, not obtainable in any other way. The values thus derived are $3d_4' = 17{,}637.11$ and $3d_1'' = 16{,}863.45$. This permits the exact calculation of an important line in the far infra-red, namely, $2p_8$-$3d_4'$ (see Table 9). The wave number of this line is $\nu = 18{,}431.77 - 17{,}637.11 = 1{,}794.66$, and the wave length 5.562 μ. An approximate value for this line can be obtained by extrapolating the $2p_8$-md_4' series to its first member. This procedure gives $\nu = 2p_8 - 3d_4' = 1{,}809.64$; which compares favorably with the exact calculation above, remembering that the approximation could be expected to yield too large a value since the calculated second member $\nu_{\text{calc.}} = 10{,}511.37$ is somewhat larger than the observed $\nu_{\text{obs.}} = 10{,}508.71$.

Furthermore, it is now possible to calculate the leading member of the $2p_9$-$3d_4$ series in the infra-red; $2p_9 - 3d_4 = 19{,}714.98 - 17{,}512.15 = 2{,}202.84$; $\lambda = 4.5396\ \mu$.

---

[31] Hund, Linienspektren und periodisches System der Elemente, p. 132, Julius Springer, Berlin; 1927.

TABLE 8.—*Xe_I fundamental series, $1s_i$-mf_k and $3d_i$-mf_k*

m	d_1'' 1 16,863.49	d_4 3 17,511.89	d_4' 4 17,636.85	d_5 1 17,847.94	d_6 0 18,063.13	s_2 1 20,649.44	s_3 0 21,637.74	s_4 1 29,789.34	s_5 2 30,766.98		
4				(1)10,853.26	(2)11,068.50	(5)13,654.73	(40)14,643.04	(10)22,794.73	(3)23,772.45	6,994.68	
5				(2)13,375.97	(2)13,591.45	(7)16,177.65	(20)17,165.91	(1)25,317.65		4,471.82	
6				(3)14,748.27	(3)14,963.65	(3)17,549.96	(4)18,538.31			3,099.40	mX
7				(3)15,574.62	(2)15,790.01	(1)18,376.58	(2)19,364.48			2,273.04	$j=1$
8					(1)16,325.65	(1)18,912.29	(1)19,899.56			1,737.83	
9						(1−)19,279.82				1,369.62	
4		(2)10,526.79		(2)10,862.89		(5)13,664.39		(15)22,804.35	(10)23,781.95	6,985.03	
5		(2*d*)13,043.58		(3)13,379.72		(9)16,181.21		(5)25,320.92	(3)26,298.45	4,468.35	
6		(2)14,414.42		(4)14,750.56		(5)17,552.12		(2)26,691.57	(2)27,669.43	3,097.50	mY
7		(2)15,239.75		(2)15,575.74		(1)18,377.60		(2)27,516.51		2,272.14	$j=2$
8		(1)15,774.74				(1)18,912.29				1,737.15	
9						(1−)19,279.82				1,369.62	
4	(1)9,891.22		(5)10,664.12				(1−)			6,972.73	
5	(8)12,407.78		(8)13,180.88							4,455.97	
6	(3)13,774.22		(2)14,547.59							3,089.26	mZ
7	(3)14,597.23		(15*d*)15,370.54							2,266.31	$j=3$
8	(2)15,130.42		(3)15,903.93							1,732.92	
9	(1)15,495.76		(1)16,269.14							1,367.71	
10	(1−)15,756.61		(1)16,530.10							1,106.75	
4		(3)10,584.59							(30)23,839.63	6,927.30	
5		(4)13,078.78							(10)26,333.78	4,433.20	
6		(5)14,435.37							(3)27,690.51	3,076.37	mU
7		(5)15,253.26							(1)28,508.31	2,258.67	$j=3$
8		(2)15,783.76							(1−)29,038.09	1,728.89	
9		(1)16,147.24								1,364.65	
4		(11)10,587.96		(1)10,923.54		(4)13,725.04		(3)22,865.11	(1)13,842.62	6,924.40	
5		(15)13,081.95		(1)13,417.29		(15*d*)16,219.33				4,430.38	mV
6				(2)14,773.40		(2)17,574.98				3,074.46	$j=2$
7				(1)15,590.73		(1)18,392.13				2,257.26	
4			(1)10,747.64							6,889.21	
5	(3)12,450.42		(2)13,224.26							4,412.59	
6	(1)13,799.21		(3)14,572.91							3,063.94	mW
7	(1)14,613.08		(1)15,386.71							2,250.14	$j=3$
8	(1)15,140.92		(1)15,914.86							1,721.99	

TABLE 9.—*Determination of $3d_4'$ and $3d_2''$*

Series, $3d_4'$-mZ

$$\nu = A - \frac{R}{[m+\mu+a(A-\nu)]^2}$$

$R_{Xe} = 109{,}736.66$
$A = 17{,}637.112$
$a = +0.000001918490443$
$\mu = +0.9538523722 \pm 10^{-10}$

M	Int.	$\lambda_{obs.}$	$\nu_{obs.}$	$\nu_{calc.}$	$\nu_{obs.} - \nu_{calc.}$
3	5	9, 374. 67	10, 664. 12	10, 664. 80	−0. 68
4	8	7, 584. 66	13, 180. 88	13, 180. 88	0. 00
5	20	6, 872. 10	14, 547. 59	14, 547. 59	0. 00
6	15*d*	6, 504. 16	15, 370. 54	15, 370. 60	−0. 06
7	3	6, 286. 02	15, 903. 93	15, 903. 97	−0. 04
8	1	6, 144. 91	16, 269. 14	16, 269. 14	0. 00
9	1−	6, 047. 9	16, 530. 10	16, 529. 93	+0. 17

$3d_4' = 17{,}637.11$

Series, $3d_2''$-mZ

$A = 16{,}863.453$
$a = +0.000001943114582$
$\mu = +0.954056552 \pm 10^{-10}$

M	Int.	$\lambda_{obs.}$	$\nu_{obs.}$	$\nu_{calc.}$	$\nu_{obs.} - \nu_{calc.}$
3	1	10, 107. 2	9, 891. 22	9, 892. 45	−1. 23
4	8	8, 057. 25	12, 407. 78	12, 407. 78	0. 00
5	3	7, 257. 94	13, 774. 22	13, 774. 22	0. 00
6	3	6, 848. 73	14, 597. 23	14, 597. 11	+0. 12
7	2	6, 607. 38	15, 130. 42	15, 130. 42	0. 00
8	1	6, 451. 6	15, 495. 76	15, 495. 55	+0. 21
9	1−	6, 344. 79	15, 756. 61	15, 756. 41	+0. 20

$3d_2'' = 16{,}863.45$

5. THE SUBORDINATE SERIES

All the observed combinations of ms_1 and md_1 levels with the mp_k− terms are collected in Table 10. It is seen from this table that some of the combinations which can be expected on the basis of assigned inner quantum numbers have not been observed, some on account of faintness, and others because they lie in the unexplored infra-red. Especially the combinations with the non-Ritzian group $2p_{1,2,3,4}$ lie far outside the range of photographic investigations. Radiometric investigations of the infra-red spectra of both krypton and xenon are desirable and important.

TABLE 10.—Xe_I *subordinate series*

m	p_5 0 17, 715. 59	p_6 2 18, 622. 04	p_7 1 18, 878. 50	p_8 3 19, 431. 51	p_9 2 19, 714. 72	p_{10} 1 20, 565. 33		
3		(2)11, 719. 93			(3)12, 812. 65		6, 902. 07	ms_4 $j=1$
4		(1)14, 209. 65	(3)14, 466. 12		(10)15, 302. 33	(1)16, 153. 08	4, 412. 35	
5			(1)15, 831. 24		(3)16, 667. 42	(4)17, 518. 11	3, 047. 28	
6			(1−)16, 635. 96		(1)17, 471. 27		2, 242. 54	
3		(2)11, 592. 12	(1)11, 848. 46	(7)12, 401. 49	(2)12, 684. 78	(5)13, 535. 44	7, 029. 96	ms_5 $j=2$
4		(2)14, 185. 84		(15)14, 995. 23	(5)15, 278. 55	(8)16, 129. 13	4, 436. 21	
5		(2)15, 547. 69		(5)16, 357. 22	(2)16, 640. 43	(2)17, 490. 80	3, 074. 36	
6		(1)16, 366. 06		(1)17, 175. 84	(1)17, 459. 37		2, 255. 67	
4		(2)10, 322. 11		(2)11, 131. 64	(3)11, 414. 83		8, 299. 90	md_1' $j=3$
5		(6)15, 521. 18		(10)14, 330. 57	(1)14, 613. 08		5, 101. 14	
6		(20)15, 157. 58		(5)15, 967. 02	(2)16, 250. 31		3, 464. 47	
7		(4)16, 122. 34		(2)16, 931. 78	(1)17, 215. 24		2, 199. 72	
8		(2)16, 734. 33		(1)17, 543. 93			1, 887. 64	
9		(1)17, 146. 50					1, 475. 54	
10		(1−)17, 436. 83					1, 184. 64	
5		(3)13, 509. 10	(1)13, 765. 57	(3)14, 318. 52	(10)14, 601. 83	(40)15, 452. 38	5, 112. 94	md_1'' $j=2$
6		(1)15, 127. 17	(15)15, 383. 43	(1)15, 936. 56	(15*d*)16, 219. 82	(2)17, 070. 53	3, 494. 90	
7			(5)16, 357. 22		(3)17, 193. 66	(1−)18, 044. 89	2, 521. 17	
8			(1)16, 975. 80		(1)17, 812. 44		1, 902. 54	
9			(1)17, 392. 24		(1−)18, 229. 15		1, 485. 91	
4			(1)10, 287. 07		(3)11, 123. 50	(2)11, 974. 24	8, 591. 24	md_5 $j=1$
5		(?)	(2)13, 758. 00		(3)14, 594. 37	(20)15, 544. 96	5, 120. 42	
6		(10)15, 073. 27	(5)15, 329. 67			(15)17, 016. 51	3, 548. 81	
7		(3)16, 062. 12	(2)16, 318. 51			(4)18, 005. 47	2, 559. 92	
8		(1)16, 692. 36				(2)18, 635. 72	1, 929. 64	
9		(1)17, 116. 80				(1)19, 059. 76	1, 505. 40	
10		(1)17, 416. 72					1, 205. 32	

TABLE 10.—*Xe_I subordinate series*—Continued

m	p_5 0 17, 715. 59	p_6 2 18, 622. 04	p_7 1 18, 878. 50	p_8 3 19, 431. 51	p_9 2 19, 714. 72	p_{10} 1 20, 565. 33		
4				(2)10, 621. 98	(5)10, 905. 13		8, 809. 56	md_4 $j=3$
5		(1)13, 433. 84		(3)14, 243. 20	(60)14, 526. 32		5, 188. 33	
6				(5)15, 887. 25	(20)16, 170. 46		3, 544. 26	
7				(2)16, 880. 07	(6)17, 163. 23		2, 551. 44	
8				(1)17, 509. 52	(3)17, 792. 47		1, 922. 12	
9					(2)18, 214. 77		1, 499. 95	
10					(1)18, 512. 01		1, 202. 71	
4				(3)10, 508. 71			8, 922. 80	md_4' $j=4$
5				(30)14, 041. 91			5, 389. 60	
6				(30)15, 823. 22			3, 608. 29	
7				(8)16, 846. 98			2, 584. 53	
8				(3)17, 489. 48			1, 942. 03	
9				(1)17, 918. 88			1, 512. 63	
10				(1—)18, 220. 18			1, 211. 33	
4						(8)11, 280. 66	9, 284. 67	md_2 $j=1$
5		(2)13, 466. 12	(5)13, 722. 51		(7)14, 558. 79	(20)15, 409. 41	5, 155. 94	
6		(3)15, 015. 61	(2)15, 272. 16		(2)16, 108. 45	(15)16, 958. 87	3, 606. 38	
7		(1)16, 016. 14			(1)17, 108. 59	(4)17, 959. 31	2, 606. 01	
8						(2)18, 644. 14	1, 921. 19	
9						(1)19, 045. 96	1, 519. 37	
5						(40)14, 990. 78	5, 574. 55	md_6 $j=0$
6						(8)16, 855. 25	3, 710. 08	
7			(1)15, 168. 58			(3)17, 910. 73	2, 654. 60	
8						(2)18, 531. 64	2, 033. 69	
9						(1)19, 059. 76	1, 505. 57	

The following additional combinations (Table 11), give a plausible explanation for an outstanding group of lines in the longer wave-length region, but one or more permitted combinations are absent in each row or column.

TABLE 11.—*Additional s'p combinations*

j		s_1''	s_1''''	s_1'''	s_1'
		2	3	2 (1)	1
	Term	6, 387. 01	6, 087. 89	5, 706. 16	5, 574. 55
1	p_{10}			(50) 14, 859. 15	(40) 14,990. 78
2	p_9	(2) 13, 327. 71	(4) 13, 626. 85		
3	p_8	(2*d*) 13, 043. 58	(2) 13, 343. 60		
1	p_7				
2	p_6	(3) 12, 235. 01		(2) 12, 915. 88	
0	p_5			(2) 12, 009. 29	

6. THE Xe_I SPECTRUM IN THE EXTREME ULTRA-VIOLET

The following lines in the extreme ultra-violet (Table 12) have been reported by Abbink and Dorgelo [32] as characteristic of the first spectrum of xenon.

TABLE 12.—*First spectrum of Xe in the extreme ultra-violet*

Line No.	Intensity	Wave length λ	Wave No. ν	Combination	Calculated term
1	20	1, 469. 61	68, 045. 3	p_0-$1s_4$	29, 798. 0
2	10	1, 295. 56	77, 186. 7	p_0-$1s_2$	20, 648. 6
3	6	[a] 1, 277. 50	78, 277. 9		19, 557. 4
4	5	1, 250. 24	79, 984. 6	p_0-$3d_5$	17, 850. 7
5	5	1, 192. 02	83, 891. 2	p_0-$2s_4$	13, 944. 1
6	15	[a] 1, 100. 46	90, 871. 1		6, 964. 2
7	10	1, 088 94	91, 832. 4		6, 002. 9
8	4	1, 083. 89	92, 260. 3	p_0-$3s_1'$	5, 575. 0
9	15	1, 074. 50	93, 066. 5	p_0-$2s_2$	4, 768. 8
10	5	1, 067. 10	93, 711. 9		4, 123. 4
11	10	1, 048. 18	95, 403. 5		2, 431. 8
12	12	1, 041. 30	96, 033. 8		1, 800. 5
13	8	1, 037. 71	96, 366. 0		1, 469. 3
14	8	1, 032. 51	96, 857. 4		783. 9
15	10	1, 027. 04	97, 367. 2		468. 1

[a] Adherence to Xe doubtful.

[32] Abbink and Dorgelo, Zeit. f. Phys., **47**, p. 221; 1928.

Since all true Xe_I lines in the extreme ultra-violet must be combinations involving the normal level $p_0 = 97{,}835.3$, it is possible to calculate the combining levels, all of which must have the inner quantum number $j = 1$. The first two levels give the resonance lines; they have been used for determining the normal state. The calculated level 17,850.7 is, without doubt, our level 17,847.94, identified as $3d_5$. The level 5,575.0 may be identified with $3s_1' = 5{,}574.55$. The levels 13,944.1 and 4,768.8 may be identified with $2s_4$ and $2s_2$, respectively, because they have a separation of 9,175.3; the separation $1s_4$-$1s_2$ is 9,139.90, and this term difference is expected to increase with higher terms approaching the $^2P_{2,1}$ interval, 9,621, in the limit.

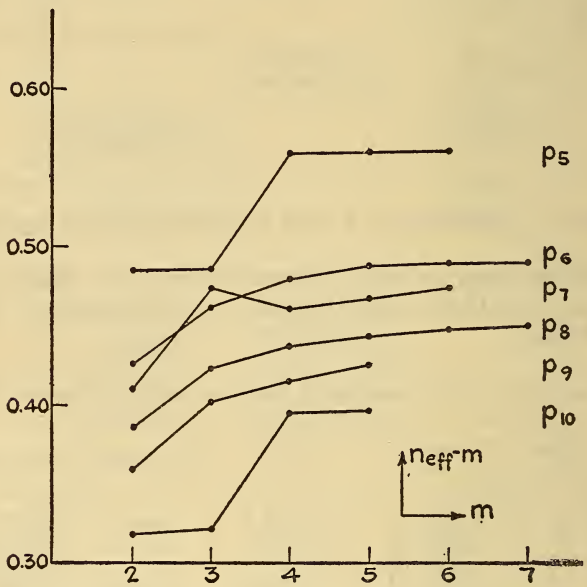

FIGURE 6.—*Effective quantum numbers for p-terms*

At this point we may also refer to the $2s_3$ level; it must be a little larger than $2s_2$, and the combination with $2p_{10}$ should have a wave number of about 15,700 cm^{-1}. Now, the only unclassified line in this region is $\nu = 15{,}729.52$. which is accordingly interpreted as $2p_{10}$-$2s_3$. The only other possible *sp* combination is $2p_7$-$2s_3$ ($\nu_{calc.} = 14{,}042.74$), which unfortunately is masked by the strong line $2p_8$-$5d'_4$ ($\nu_{obs.} = 14{,}041.91$).

In the case of Kr_I, it was possible to account for all the extreme ultra-violet lines, but it is seen from Table 12 that a considerable number of strong lines attributed to the Xe_I spectrum by Abbink and Dorgelo remains unclassified. It appears that another interpretation will have to be sought for the remaining lines.

7. IDENTIFICATION OF THE EXPERIMENTAL TERMS

A complete list of the identified Xe_I terms is presented in Table 13. The first column contains the type of electron which, when added to s^2p^5, gives rise to groups of terms shown in the second column (Paschen notation), followed by the inner quantum numbers assigned

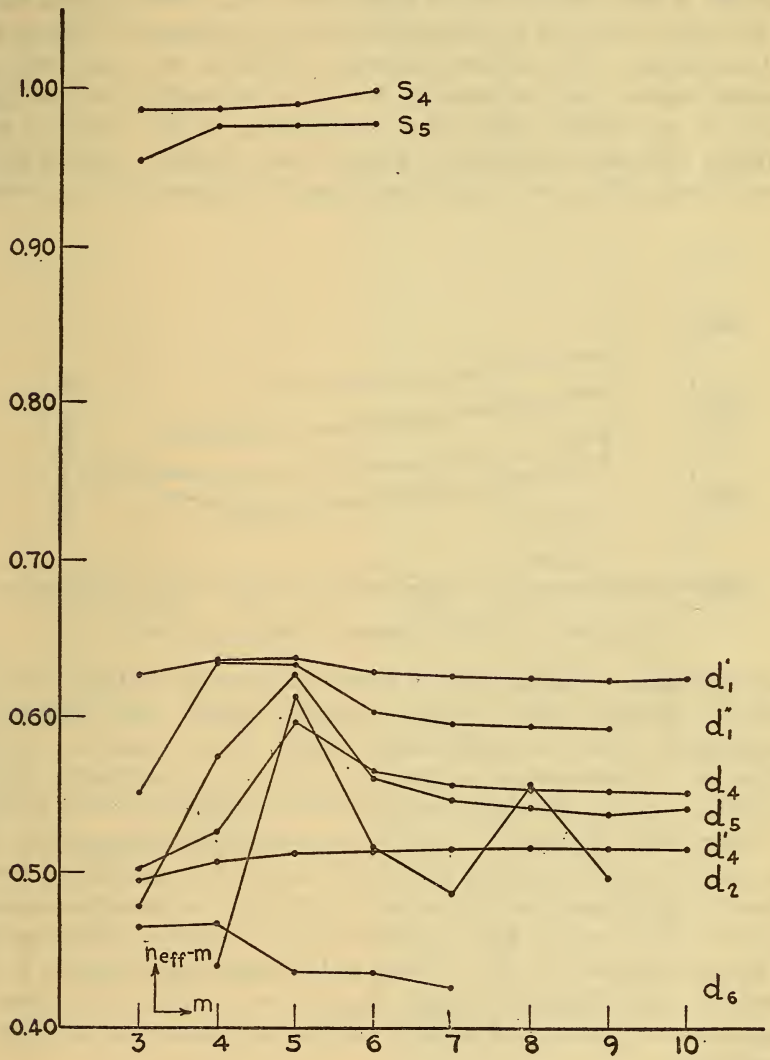

FIGURE 7.—*Effective quantum numbers for d- and s-terms*

to the terms. The absolute value of the ground level or highest term appears in column 4, and the remaining columns contain alternately the term values and the corresponding effective quantum numbers. The latter are an excellent criterion for arranging terms in series, and when they are plotted as a function of order number they reveal

certain relations and regularities not otherwise obvious. Such plots are shown in Figures 6, 7, and 8, p-terms in Figure 6, d- and s'-terms in Figure 7, and f-terms in Figure 8. The order numbers (m) of the terms in the series are taken for abscissæ and the fractional part of the corresponding effective quantum numbers (n_{eff}-m) as ordinates. On account of the relatively small departures of n_{eff} from integral values in the cases of f-terms an expanded scale was necessary in Figure 8.

Comparison with similar diagrams published for other rare gas spectra shows that, in general, the series converging to the upper limit $^2P_1$ are shorter than those coordinated to $^2P_2$. This is most striking with the heavier gas; whereas two members each of $p_{1,2,3,4}$ were found in Kr_I, only one of each can be detected in Xe_I because

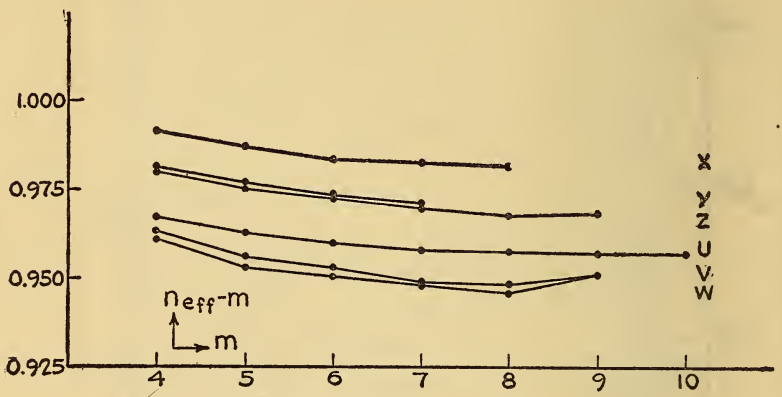

FIGURE 8.—*Effective quantum numbers for f-terms*

the separation of the groups of terms has become so large that the second members would acquire negative values. The behavior of homologous terms is remarkably similar in all rare gas spectra Thus, in each case certain p-terms (p_6, p_7, and p_8, p_9) are fairly regular, whereas p_5 and p_{10} are most irregular but nevertheless remain parallel.

Comparison of Figure 7 with the corresponding diagrams for Ne_I A_I, and Kr_I calls attention to the fact that in all cases the d'_4 series gives the most nearly perfect smooth curves, but whereas the constant α of the Ritz formula has a positive value in the first three spectra it becomes negative in Xe_I. Most of the remaining d-series are very irregular and dissimilar except that for $m=5$ they all appear to experience in greater or smaller degree the same perturbation or resonance.

The curves for the f-terms (fig. 8) show no large discontinuities; they behave more like the hydrogen series, as would be expected if they really involve the larger f-orbits.

Electron		
p	6. 9749	
s	6. 9953	
	6. 4498	1
	6. 4742	
p	6. 4905	1
	6. 5618	
	5. 4386	2
	5. 5147	2
	5. 5643	2
	5. 5162	2
	5. 5608	2
d	5. 6035	2
	5. 6280	2
	5. 9503	2
	5. 9521	2
f	5. 9601	2
	5. 9725	2
	5. 9744	2
	5. 9847	2

TABLE 13.—*Terms and effective quantum numbers of Xe* I

Series	j	Paschen notation		$m=$ 1		2		3		4		5		6		7		8		9		10	
p	0	p_0	97, 835. 3																				
s	2	s_5		30, 766. 98	1. 8886			7, 029. 96	3. 9510	4, 436. 21	4. 9736	3, 074. 36	5. 9745	2, 255. 67	6. 9749								
	1	s_4		29, 789. 34	1. 9193	13, 944. 1	2. 8054	6, 902. 07	3. 9874	4, 412. 35	4. 9851	3, 047. 28	6. 0010	2, 242. 54	6. 9953								
	0	s_3		21, 637. 74	1. 8736	4, 835. 76	2. 7552																
	1	s_2		20, 649. 44	1. 9040	4, 768. 8	2. 7617																
p	1	p_{10}				20, 565. 33	2. 3100	9, 907. 29	3. 3281	5, 681. 21	4. 3950	3, 767. 26	5. 3972										
	2	p_9				19, 714. 72	2. 3593	9, 482. 80	3. 4018	5, 613. 10	4. 4216	3, 724. 37	5. 4281										
	3	p_8				19, 431. 51	2. 3764	9, 365. 27	3. 4231	5, 569. 61	4. 4388	3, 700. 06	5. 4459	2, 637. 91	6. 4498	1, 976. 92	7. 4504						
	1	p_7				18, 878. 50	2. 4110	9, 089. 92	3. 4743	5, 501. 53	4. 4661	3, 665. 64	5. 4714	2, 618. 04	6. 4742								
	2	p_6				18, 622. 04	2. 4275	9, 147. 97	3. 4635	5, 463. 48	4. 4817	3, 644. 40	5. 4874	2, 604. 93	6. 4905	1, 956. 43	7. 4893						
	0	p_5				17, 715. 59	2. 4888	8, 992. 20	3. 4933	5, 279. 09	4. 5593	3, 549. 35	5. 5604	2, 548. 67	6. 5618								
	1	p_4				9, 455. 37	2. 3984																
	2	p_3				8, 672. 18	2. 4492																
	1	p_2				8, 555. 78	2. 4571																
	0	p_1				7, 974. 43	2. 4973																
d	0	d_5						18, 063. 13	2. 4648	9, 125. 98	3. 4677	5, 574. 55	4. 4368	3, 710. 08	5. 4386	2, 654. 60	6. 4295	2, 033. 69	7. 3457	1, 505. 57	8. 5374		
	4	d_4'						17, 636. 85	2. 4944	8, 922. 80	3. 5070	5, 389. 60	4. 5122	3, 608. 29	5. 5147	2, 584. 53	6. 5160	1, 942. 03	7. 5171	1, 512. 63	8. 5174	1, 214. 83	9. 5160
	3	d_4						17, 511. 89	2. 5033	8, 809. 56	3. 5295	5, 188. 33	4. 5990	3, 544. 26	5. 5643	2, 551. 44	6. 5582	1, 922. 12	7. 5559	1, 499. 95	8. 5534	1, 202. 71	9. 5520
	1	d_2								9, 284. 67	3. 4379	5, 155. 94	4. 6134	3, 606. 38	5. 5162	2, 606. 01	6. 4891	1, 921. 19	7. 5577	1, 519. 37	8. 4985		
	1	d_5						17, 847. 94	2. 4796	8, 591. 24	3. 5740	5, 120. 42	4. 6294	3, 548. 81	5. 5608	2, 559. 92	6. 5473	1, 929. 64	7. 5412	1, 505. 40	8. 5378	1, 205. 32	9. 5417
	2	d_1''						16, 863. 49	2. 5510	8, 289. 42	3. 6365	5, 112. 94	4. 6328	3, 494. 90	5. 6035	2, 521. 17	6. 5974	1, 902. 54	7. 5947	1, 485. 91	8. 5936		
	3	d_1'						15, 907. 90	2. 6264	8, 299. 90	3. 6362	5, 101. 14	4. 6381	3, 464. 47	5. 6280	2, 499. 72	6. 6257	1, 887. 64	7. 6246	1, 475. 54	8. 6238	1, 184. 64	9. 6246
	2	s_1''						6, 387. 01	2. 6182														
	3	s_1''''						6, 087. 89	2. 6430														
	2	s_1'''						5, 706. 16	2. 6757														
	1	s_1'						5, 574. 55	2. 6823														
f	1	$X(f_6)$								6, 994. 68	3. 9609	4, 471. 82	4. 9538	3, 099. 40	5. 9503	2, 273. 04	6. 9482	1, 737. 83	7. 9464	1, 369. 62	8. 9510		
	2	$Y(f_5)$								6, 985. 03	3. 9636	4, 468. 35	4. 9557	3, 097. 50	5. 9521	2, 272. 44	6. 9496	1, 737. 45	7. 9480	1, 369. 62	8. 9510		
	3	$Z(f_4)$								6, 972. 73	3. 9671	4, 455. 97	4. 9626	3, 089. 26	5. 9601	2, 266. 31	6. 9586	1, 732. 92	7. 9577	1, 367. 74	8. 9573	1, 106. 75	9. 9575
	3	$U(f_3)$								6, 927. 30	3. 9801	4, 433. 20	4. 9753	3, 076. 37	5. 9725	2, 258. 67	6. 9703	1, 728. 89	7. 9670	1, 364. 65	8. 9674		
	2	$V(f_2)$								6, 924. 40	3. 9810	4, 430. 38	4. 9769	3, 074. 46	5. 9744	2, 257. 26	6. 9724						
	3	$W(f_1)$								6, 889. 21	3. 9911	4, 412. 59	4. 9869	3, 063. 94	5. 9847	2, 250. 14	6. 9835	1, 721. 99	7. 9829				

8. LIST OF Xe_I LINES

A complete list of the observed lines characteristic of the first spectrum of xenon is presented in Table 14, in which the estimated intensities appear in the first column, the wave lengths (international scale) in the second, wave numbers (vacuum) in the third, and term combinations in the last. Practically all of the 318 observed lines are accounted for as combinations of established terms presented in the preceding table. Only a few lines, most of which are very faint, remain unclassified; it will perhaps be possible to place them when related, but still fainter lines have been recorded.

TABLE 14.—*List of Xe_I lines*

Intensity	Wave length	Wave number	Combination
1	10, 107. 2	9, 891. 22	$3d_1''$-$4Z$
10	9, 923. 10	10, 074. 74	$1s_4$-$2p_9$
20	9, 799. 65	10, 201. 65	$1s_5$-$2p_{10}$
1	9, 718. 27	10, 287. 07	$2p_6$-$4d_5$
2	9, 685. 29	10, 322. 11	$2p_6$-$4d_1'$
6	9, 513. 34	10, 508. 67	$2p_8$-$4d_4'$
2	9, 496. 97	10, 526. 79	$3d_4$-$4Y$
3	9, 445. 34	10, 584. 37	$3d_4$-$4U$
1—	9, 442. 1	10, 587. 96	$3d_4$-$4V$
2	9, 411. 86	10, 621. 98	$2p_8$-$4d_4$
5	9, 374. 67	10, 664. 12	$3d_4'$-$4Z$
1	9, 306. 56	10, 742. 17	$1s_2$-$3p_{10}$
1	9, 301. 82	10, 747. 64	$3d_4'$-$4W$
1	9, 211. 3	10, 853. 26	$3d_5$-$4X$
2	9, 203. 13	10, 862. 89	$3d_5$-$4Y$
5	9, 167. 48	10, 905. 13	$2p_9$-$4d_4$
40	9, 162. 66	10, 910. 87	$1s_4$-$2p_7$
1	9, 152. 03	10, 923. 54	$3d_5$-$4V$
1	9, 095. 57	10, 990. 87	
50	9, 045. 46	11, 052. 24	$1s_5$-$2p_9$
2	9, 032. 17	11, 068. 50	$3d_6$-$4X$
1	9, 025. 74	11, 076. 38	
3	8, 987. 51	11, 123. 50	$2p_9$-$4d_5$
2	8, 980. 94	11, 131. 64	$2p_8$-$4d_1'$
50	8, 952. 25	11, 167. 31	$\left\{ \begin{array}{l} 1s_2\text{-}3p_9 \\ 1s_4\text{-}2p_6 \end{array} \right.$
5	8, 930. 81	11, 194. 03	$1s_3$-$2p_4$
1	8, 913. 33	11, 216. 08	
4	8, 908. 70	11, 221. 91	
8	8, 862. 30	11, 280. 66	$2p_{10}$-$4d_2$
200	8, 819. 44	11, 335. 47	$1s_5$-$2p_8$
3	8, 758. 13	11, 414. 83	$2p_9$-$4d_1'$
10	8, 739. 36	11, 439. 35	$2p_{10}$-$4d_6$
1	8, 725. 4	11, 457. 65	
1	8, 709. 6	11, 478. 43	$3d_1'$-$5V$?
3	8, 696. 80	11, 495. 33	$3d_1'$-$5W$
3	8, 692. 08	11, 501. 57	$1s_3$-$3p_6$
6	8, 648. 51	11, 559. 51	$1s_2$-$3p_7$
2	8, 624. 18	11, 592. 12	$2p_6$-$3s_5$
5	8, 576. 03	11, 657. 21	$1s_2$-$3p_5$
2	8, 530. 13	11, 719. 93	$2p_6$-$3s_4$

TABLE 14.—*List of Xe_I lines*—Continued

Intensity	Wave length	Wave number	Combination
2	8, 522. 49	11, 730. 44	$1s_3$-$3p_{10}$
1	8, 437. 6	11, 848. 46	$2p_7$-$3s_5$
60	8, 409. 21	11, 888. 46	$1s_5$-$2p_7$
1	8, 392. 4	11, 912. 27	
1	8, 368. 4	11, 946. 44	
2	8, 348. 97	11, 974. 24	$2p_7$-$3s_4$ $2p_{10}$-$4d_5$
50	8, 346. 86	11, 977. 26	$1s_2$-$2p_3$
2	8, 324. 6	12, 009. 26	$2p_5$-s_1'''
2	8, 319. 46	12, 016. 71	
150	8, 280. 16	12, 073. 75	$1s_4$-$2p_5$
20	8, 266. 53	12, 093. 65	$1s_2$-$2p_2$
1	8, 258. 0	12, 106. 15	
300	8, 231. 64	12, 144. 92	$1s_5$-$2p_6$
1?	8, 228. 7	12, 149. 25	
25	8, 206. 34	12, 182. 36	$1s_3$-$2p_4$
1	8, 191. 7	12, 204. 13	
3	8, 171. 02	12, 235. 01	$3d_5$-$4p_9$
2	8, 143. 8	12, 275. 91	
2	8, 101. 95	12, 339. 32	
7	8, 061. 33	12, 401. 49	$2p_8$-$3s_5$
8	8, 057. 25	12, 407. 78	$3d_1''$-$5Z$
3	8, 029. 65	12, 450. 42	$3d_1''$-$5W$
10	7, 967. 33	12, 547. 81	$1s_3$-$3p_7$
1	7, 937. 47	12, 595. 02	$2p_5$-$5d_5$
8	7, 887. 38	12, 675. 00	$1s_2$-$2p_1$
2	7, 881. 30	12, 684. 78	$2p_9$-$3s_5$
3	7, 802. 64	12, 812. 65	$2p_9$-$3s_4$
2	7, 783. 63	12, 843. 94	$3d_1'$-$6W$
2	7, 740. 28	12, 915. 88	$2p_6$-s_1'''
2*d*	7, 664. 5	13, 043. 58	$3d_4$-$5Y$ $2p_8$-s_1''
4	7, 643. 87	13, 078. 78	$3d_4$-$5U$
15	7, 642. 02	13, 081. 95	$1s_3$-$2p_2$ $3d_4$-$5V$
1—	7, 587. 6	13, 175. 78	
8	7, 584. 66	13, 180. 88	$3d_4'$-$5Z$
2	7, 559. 78	13, 224. 26	$3d_4'$-$5W$
2	7, 501. 10	13, 227. 71	$2p_9$-s_1''
2	7, 492. 17	13, 343. 60	$2p_8$-s_1''''
2	7, 474. 04	13, 375. 97	$3d_5$-$5X$
3	7, 471. 94	13, 379. 72	$3d_5$-$5Y$
1	7, 451. 02	13, 417. 29	$3d_5$-$5V$
1	7, 441. 84	13, 433. 84	$2p_6$-$5d_4$
2	7, 424. 0	13, 466. 12	$2p_6$-$5d_2$
3	7, 400. 38	13, 509. 10	$2p_6$-$5d_1''$
6	7, 393. 77	13, 521. 18	$2p_6$-$5d_1''$
5	7, 385. 98	13, 535. 44	$2p_{10}$-$3s_5$
2	7, 355. 54	13, 591. 45	$3d_6$-$5X$
4	7, 336. 44	13, 626. 85	$2p_9$-s_1''
5	7, 321. 46	13, 654. 73	$1s_2$-$4X$
5	7, 316. 28	13, 664. 39	$1s_2$-$4Y$

TABLE 14.—*List of Xe_I lines*—Continued

Intensity	Wave length	Wave number	Combination
5	7, 285. 29	13, 722. 51	$2p_7$-$4d_2$
4	7, 283. 95	13, 725. 04	$1s_2$-$4V$
2	7, 266. 50	13, 758. 00	$2p_7$-$5d_5$
1	7, 262. 5	13, 765. 57	$2p_7$-$5d_1''$
3	7, 257. 94	13, 774. 22	$3d_1''$-$6Z$
1	7, 244. 8	13, 799. 21	$3d_1''$-$6W$
30	7, 119. 58	14, 041. 91	$2p_7$-$2s_3$ $2p_8$-$5d_4'$
2	7, 047. 34	14, 185. 84	$2p_6$-$4s_5$
1	7, 035. 53	14, 209. 65	$2p_6$-$4s_4$
3	7, 018. 96	14, 243. 20	$2p_8$-$5d_4$
3	6, 982. 04	14, 318. 52	$2p_8$-$5d_1''$
10	6, 976. 17	14, 330. 57	$2p_8$-$5d_1'$
2	6, 935. 59	14, 414. 42	$3d_4$-$6Y$
5	6, 925. 52	14, 435. 37	$3d_4$-$6U$
3	6, 910. 80	14, 466. 12	$2p_7$-$4s_4$
60	6, 882. 16	14, 526. 32	$2p_9$-$5d_4$
20	6, 872. 10	14, 547. 59	$3d_4'$-$6Z$
7	6, 866. 81	14, 558. 79	$2p_9$-$5d_2$
1	6, 863. 21	14, 566. 43	
3	6, 860. 16	14, 572. 91	$3d_4'$-6W
3	6, 850. 07	14, 594. 37	$2p_9$-$5d_5$
3	6, 848. 73	14, 597. 23	$3d_1''$-$7Z$
10	6, 846. 57	14, 601. 83	$2p_9$-$5d_1''$
1	6, 841. 30	14, 613. 08	$3d_1''$-$7W$ $2p_9$-$5d_1'$
40	6, 827. 30	14, 643. 04	$1s_3$-$4X$
1	6, 818. 30	14, 662. 37	
3	6, 778. 59	14, 748. 27	$3d_5$-$6X$
4	6, 777. 53	14, 750. 56	$3d_5$-$6Y$
2	6, 767. 06	14, 773. 40	$3d_5$-$6V$
50	6, 728. 00	14, 859. 16	
3	6, 681. 02	14, 963. 65	$3d_6$-$6Z$
4	6, 678. 94	14, 968. 31	$1s_2$-$4p_{10}$
40	6, 668. 93	14, 990. 78	$2p_{10}$-$5d_6$
15	6, 666. 95	14, 995. 23	$2p_8$-$4s_5$
3	6, 657. 90	15, 015. 61	$2p_6$-$6d_2$
10	6, 632. 43	15, 073. 27	$2p_6$-$6d_5$
1	6, 608. 8	15, 127. 17	$2p_6$-$6d_1''$
2	6, 607. 38	15, 130. 42	$3d_1''$-$8Z$
1	6, 602. 8	15, 140. 92	$3d_1''$-$8W$
20	6, 595. 54	15, 157. 58	$2p_6$-$6d_1'$
1	6, 590. 76	15, 168. 56	$2p_7$-$6d_6$
3	6, 583. 15	15, 186. 11	$1s_2$-$4p_6$
2	6, 559. 98	15, 239. 75	$3d_4$-$7Y$
5	6, 554. 17	15, 253. 26	$3d_4$-$7U$
2	6, 546. 06	15, 272. 16	$2p_7$-$6d_2$
5	6, 543. 32	15, 278. 55	$2p_9$-$4s_5$
10	6, 533. 15	15, 302. 33	$2p_9$-$4s_4$
5	6, 521. 50	15, 329. 67	$2p_7$-$6d_5$
15*d*	6, 504. 16	15, 370. 54	$3d_4$-$7Z$ $1s_2$-$4p_5$
1—	6, 500. 23	15, 379. 83	

TABLE 14.—*List of Xe_I lines*—Continued

Intensity	Wave length	Wave number	Combination
15	6, 498. 71	15, 383. 43	$2p_7$-$6d_1''$
1	6, 497. 3	15, 386. 76	$3d_4'$-$7W$
20	6, 487. 75	15, 409. 41	$2p_{10}$-$5d_2$
20	6, 472. 82	15, 444. 96	$2p_{10}$-$5d_5$
40	6, 469. 71	15, 452. 38	$2p_{10}$-$5d_1''$
1	6, 451. 6	15, 495. 76	$3d_1''$-$9Z$
1—	6, 450. 10	15, 499. 36	
2	6, 430. 05	15, 547. 69	$2p_6$-$5s_5$
3	6, 418. 93	15, 574. 62	$3d_5$-$7X$
2	6, 418. 47	15, 575. 74	{ $3d_5$-$7Y$ $2p_6$-$5s_4$
1	6, 412. 3	15, 590. 73	$3d_5$-$7V$
2	6, 355. 72	15, 729. 52	$2p_{10}$-$2s_3$
1—	6, 344. 79	15, 756. 61	$3d_1''$-$10Z$
1	6, 337. 5	15, 774. 74	$3d_4$-$8Y$
2	6, 333. 88	15, 783. 76	$3d_4$-$8U$
2	6, 331. 37	15, 790. 01	$3d_6$-$7Z$
30	6, 318. 08	15, 823. 23	$2p_8$-$6d_4'$
1	6, 314. 88	15, 831. 24	$2p_7$-$5s_4$
1	6, 294. 36	15, 882. 85	
5	6, 292. 62	15, 887. 25	$2p_9$-$6d_4$
3	6, 286. 02	15, 903. 93	$3d_4'$-$8Z$
1	6, 281. 7	15, 914. 86	$3d_4'$-$8W$
1	6, 277. 2	15, 926. 27	
1	6, 273. 15	15, 936. 56	$2p_8$-$6d_1''$
4	6, 265. 28	15, 956. 57	$1s_3$-$4p_{10}$
5	6, 261. 18	15, 967. 02	$2p_8$-$6d_1'$
1	6, 241. 98	16, 016. 14	$2p_6$-$7d_2$
3	6, 224. 11	16, 062. 12	$2p_6$-$7d_5$
2	6, 206. 21	16, 108. 45	{ $3d_5$-$8X$ $2p_9$-$6d_2$
4	6, 200. 86	16, 122. 34	$2p_6$-$7d_1'$
8	6, 198. 25	16, 129. 13	$2p_{10}$-$4s_5$
1?	6, 191. 3	16, 147. 24	$3d_4$-$9U$
1	6, 189. 06	16, 153. 08	$2p_{10}$-$4s_4$
20	6, 182. 41	16, 170. 46	$2p_9$-$6d_4$
7	6, 179. 66	16, 177. 66	$1s_2$-$5X$
9	6, 178. 30	16, 181. 21	$1s_2$-$5Y$
15*d*	6, 163. 78	16, 219. 33	{ $1s_2$-$5V$ $2p_9$-$6d_1''$
2	6, 152. 03	16, 250. 31	$2p_9$-$6d_1'$
1	6, 144. 91	16, 269. 14	$3d'_4$-$9Z$
1	6, 126. 32	16, 318. 51	$2p_7$-$7d_5$
1—	6, 123. 64	16, 325. 65	$3d_6$-$8X$
1	6, 114. 7	16, 349. 52	
5	6, 111. 82	16, 357. 22	{ $2p_8$-$5s_5$ $2p_7$-$7d_1''$
1—	6, 108. 52	16, 366. 06	$2p_6$-$6s_5$
1	6, 047. 9	16, 530. 10	$3d_4$-$10Z$
1	6, 043. 2	16, 542. 95	
1—	6, 009. 41	16, 635. 96	$2p_7$-$6s_4$
2	6, 007. 80	16, 640. 43	$2p_9$-$5s_5$
3	5, 998. 07	16, 667. 42	$2p_9$-$5s_4$
1	5, 989. 11	16, 692. 36	$2p_6$-$8d_5$

TABLE 14.—*List of Xe_I lines*—Continued

Intensity	Wave length	Wave number	Combination
2	5, 974. 09	16, 734. 33	$2d_5$-$10XY$ $2p_6$-$8d_1'$
10	5, 934. 15	16, 846. 96	$2p_8$-$7d_4'$
8	5, 931. 23	16, 855. 25	$2p_{10}$-$6d_6$
1—	5, 925. 33	16, 872. 03	
2	5, 922. 51	16, 880. 07	$2p_9$-$7d_4$
1	5, 921. 79	16, 882. 12	$1s_2$-$5p_{10}$
2	5, 904. 42	16, 931. 78	$2d_5$-$11XY$ $2p_8$-$7d_1'$
15	5, 894. 99	16, 958. 87	$2p_{10}$-$6d_2$
1	5, 889. 11	16, 975. 80	$2p_7$-$8d_1''$
15	5, 875. 02	17, 016. 51	$2p_{10}$-$6d_5$
2	5, 856. 43	17, 070. 53	$2p_{10}$-$6d_1''$
1—	5, 849. 47	17, 090. 83	
1	5, 843. 4	17, 108. 59	$2p_9$-$7d_2$
1	5, 840. 6	17, 116. 80	$2p_6$-$9d_5$
1	5, 830. 48	17, 146. 50	$2p_6$-$9d_1'$
6	5, 824. 78	17, 163. 28	$2p_9$-$7d_4$
20	5, 823. 89	17, 165. 91	$1s_3$-$5X$
1	5, 820. 52	17, 175. 84	$2p_8$-$6s_5$
3	5, 814. 49	17, 193. 66	$2p_9$-$7d_1''$
1	5, 807. 2	17, 215. 24	$2p_9$-$7d_1'$
1	5, 748. 1	17, 392. 24	$2p_7$-$9d_1''$
1	5, 740. 2	17, 416. 72	$2p_6$-$10d_5$
1—	5, 733. 4	17, 436. 83	$2p_6$-$10d_1'$
1	5, 726. 0	17, 459. 37	$2p_9$-$6s_5$
1	5, 722. 1	17, 471. 27	$2p_6$-$10d_5$ $2p_9$-$6s_4$
4	5, 716. 14	17, 489. 48	$2p_8$-$8d_4'$
2	5, 715. 71	17, 490. 80	$2p_{10}$-$5s_5$
1	5, 709. 6	17, 509. 52	$2p_9$-$8d_4$
1—	5, 706. 8	17, 518. 11	$2p_{10}$-$5s_4$
1—	5, 698. 4	17, 543. 93	$2p_8$-$8d_1'$
3	5, 696. 44	17, 549. 96	$1s_2$-$6X$
5	5, 695. 74	17, 552. 12	$1s_2$-$6Y$
2	5, 688. 31	17, 575. 05	$1s_2$-$6V$
3	5, 618. 80	17, 792. 47	$2p_9$-$8d_4$
1	5, 612. 5	17, 812. 44	$2p_9$-$8d_1''$
1	5, 594. 21	17, 870. 68	$1s_3$-$5p_{10}$
3	5, 581. 70	17, 910. 73	$2p_{10}$-$7d_6$
2	5, 579. 19	17, 918. 78	$2p_8$-$9d_4'$
4	5, 566. 60	17, 959. 31	$2p_{10}$-$7d_2$
4	5, 552. 33	18, 005. 47	$2p_7$-$7d_5$
1—	5, 540. 2	18, 044. 89	$1s_2$-$6p_6$ $2p_{10}$-$7d_1''$
2	5, 488. 53	18, 214. 77	$2p_9$-$9d_4$
1	5, 487. 05	18, 219. 68	$2p_8$-$10d_4'$
1—	5, 484. 2	18, 229. 15	$2p_9$-$9d_1''$
1	5, 440. 2	18, 376. 58	$1s_2$-$7X$
1	5, 439. 9	18, 377. 60	$1s_2$-$7Y$
1	5, 435. 6	18, 392. 13	$1s_2$-$7V$
1	5, 418. 0	18, 451. 88	
1	5, 400. 4	18, 512. 01	$2p_9$-$10d_4$
2	5, 394. 68	18, 531. 64	$2p_{10}$-$8d_6$

TABLE 14.—*List of Xe_I lines*—Continued

Intensity	Wave length	Wave number	Combination
4	5, 392. 74	18, 538. 31	$1s_3$-$6X$
1—	5, 368. 99	18, 620. 31	
1	5, 367. 0	18, 627. 22	
2	5, 364. 55	18, 635. 72	$2p_{10}$-$8d_5$
2	5, 362. 13	18, 644. 14	$2p_{10}$-$8d_2$
1—	5, 328. 5	18, 761. 80	
1—	5, 306. 23	18, 840. 55	
1	5, 286. 1	18, 912. 29	$1s_2$-$8Y$
1	5, 249. 0	19, 045. 96	$2p_{10}$-$9d_2$
1	5, 245. 2	19, 059. 76	$2p_{10}$-$9d_5$
1—	5, 185. 33	19, 279. 82	$1s_2$-$9Y$
2	5, 162. 66	19, 364. 48	$1s_3$-$7X$
15	5, 028. 26	19, 882. 07	$1s_4$-$3p_{10}$
1	5, 023. 84	19, 899. 56	$1s_3$-$8XY$
60	4, 923. 15	20, 306. 55	$1s_4$-$3p_9$
50	4, 916. 50	20, 334. 01	$1s_4$-$2p_4$
60	4, 843. 29	20, 641. 37	$1s_4$-$3p_6$
70	4, 829. 71	20, 669. 41	$1s_4$-$3p_7$
100	4, 807. 01	20, 797. 16	$1s_4$-$3p_5$
20	4, 792. 61	20, 859. 64	$1s_5$-$3p_{10}$
1—	4, 755. 69	21, 017. 17	
1*h*?	4, 746. 40	21, 062. 73	
100	4, 734. 15	21, 117. 23	$1s_4$-$2p_3$
2	4, 721. 01	21, 176. 00	
2	4, 708. 19	21, 233. 66	$1s_4$-$2p_2$
70	4, 697. 02	21, 284. 16	$1s_5$-$3p_9$
25	4, 690. 97	21, 311. 61	$1s_5$-$2p_4$
300	4, 671. 22	21, 401. 71	$1s_5$-$3p_8$
1	4, 636. 55	21, 561. 74	$1s_5$-$3p_6$
200	4, 624. 29	21, 618. 90	
1	4, 621. 36	21, 632. 61	
8	4, 611. 88	21, 677. 08	$1s_5$-$3p_7$
30	4, 582. 74	21, 814. 92	$1s_4$-$2p_1$
1	4, 574. 86	21, 852. 49	
50	4, 524. 68	22, 094. 83	$1s_5$-$2p_3$
100	4, 500. 99	22, 211. 12	$1s_5$-$2p_2$
10	4, 385. 75	22, 794. 73	$1s_4$-$4X$
15	4, 383. 90	22, 804. 35	$1s_4$-$4Y$
3	4, 372. 25	22, 865. 11	$1s_4$-$4V$
1	4, 215. 5	23, 715. 32	
3	4, 205. 37	23, 772. 45	$1s_5$-$4X$
10	4, 203. 69	23, 781. 95	$1s_5$-$4Y$
30	4, 193. 51	23, 839. 68	$1s_5$-$4U$
1	4, 192. 99	23, 842. 62	$1s_5$-$4V$
4	4, 135. 12	24, 176. 30	$1s_4$-$4p_9$
15	4, 116. 11	24, 287. 95	$1s_4$-$4p_7$
10	4, 109. 71	24, 325. 78	$1s_4$-$4p_6$
20	4, 078. 81	24, 510. 06	$1s_4$-$4p_5$
1	4, 057. 80	24, 636. 96	
5	3, 985. 22	25, 085. 65	$1s_5$-$4p_{10}$

TABLE 14.—*List of Xe_I lines*—Continued

Intensity	Wave length	Wave number	Combination
5	3, 974. 42	25, 153. 81	$1s_5$-$4p_9$
30	3, 967. 55	25, 197. 37	$1s_5$-$4p_8$
1	3, 956. 88	25, 265. 31	$1s_5$-$4p_7$
20	3, 950. 92	25, 303. 43	$1s_5$-$4p_6$
1	3, 948. 70	25, 317. 65	$1s_4$-$6X$
5	3, 948. 19	25, 320. 92	$1s_4$-$5Y$
1	3, 842. 4	26, 018. 05	
3	3, 826. 86	26, 123. 70	$1s_4$-$5p_7$
2	3, 823. 76	26, 144. 88	$1s_4$-$5p_6$
4	3, 809. 90	26, 239. 99	$1s_4$-$5p_5$
3	3, 801. 43	26, 298. 45	$1s_5$-$5Y$
10	3, 796. 33	26, 333. 78	$1s_5$-$5U$
2	3, 745. 44	26, 691. 57	$1s_4$-$6Y$
1	3, 702. 72	26, 999. 52	$1s_5$-$5p_{10}$
1	3, 696. 82	27, 042. 61	$1s_5$-$5p_9$
5	3, 693. 50	27, 066. 92	$1s_5$-$5p_8$
4	3, 685. 91	27, 122. 65	$1s_5$-$5p_6$
1	3, 679. 31	27, 171. 30	$1s_4$-$6p_7$
1−	3, 677. 62	27, 183. 79	$1s_4$-$6p_6$
2	3, 669. 94	27, 240. 67	$1s_4$-$6p_5$
2	3, 633. 15	27, 516. 51	$1s_4$-$7Y$
2	3, 613. 07	27, 669. 43	$1s_5$-$6Y$
3	3, 610. 32	27, 690. 51	$1s_5$-$6U$
2	3, 554. 03	28, 129. 07	$1s_5$-$6p_8$
2	3, 549. 84	28, 162. 27	$1s_5$-$6p_6$
1	3, 506. 75	28, 508. 31	$1s_5$-$7U$
1	3, 472. 43	28, 790. 06	$1s_5$-$7p_8$
1	3, 469. 96	28, 810. 55	$1s_5$-$7p_6$
1−	3, 442. 77	29, 038. 09	$1s_5$-$8U$

The general features of this classification of Xe_I lines parallel those of the preceding rare gases, Ne_I, A_I, Kr_I, and are also in accord with the structure expected on theoretical grounds. Many resemblances among these four spectra have been alluded to in this paper, but we shall reserve further discussion and interpretation of them so as to include comparisons with the fifth spectrum, that of radon, which is now under investigation.

The cooperation of the authors has been made possible in this investigation through the grant of a research fellowship to one of them (T. L. deB.) by the International Education Board.

WASHINGTON, May 10, 1929.